REPUBLIC OF AZERBAIJAN

On the right of the manuscript

ABSTRACT

of the dissertation for the degree of Doctor of Science

PHYSICO-CHEMICAL BASES FOR OBTAINING THALLIUM TELLURIDES WITH RARE EARTH ELEMENTS AND MULTICOMPONENT PHASES BASED ON THEM

Specialty: 2303.01 – inorganic chemistry

Field of science: chemistry

Applicant: Samira Zakir Imamaliyeva

Baku – 2022

The dissertation was carried out in the "Thermodynamics of functional inorganic compounds" laboratory of the "Functional inorganic materials" department of the Institute of Catalysis and Inorganic Chemistry named after acad. M.Nagiyev of Azerbaijan National Academy of Sciences.

Scientific consultant: Corr.-member of ANAS, professor **Mahammad Baba Babanly**

Official opponents D. Sci. Chem., professor **Ozbek Misirkhan Aliev**

Corr.-member of ANAS, professor **Tofig Abbasali Aliyev**

D. Sci. Chem., professor **Alexandr Yuriyevich Zavrajnov**

D. Sci. Chem., professor **Huseyn Ramazan Gurbanov**

Dissertation council ED1.15 of Supreme Attestation Commission under the President of the Republic of Azerbaijan operating at acad.M.Naghiyev Institute of Catalysis and Inorganic Chemistry

Chairman of the Dissertation council

Academician **Dilgam Babir Taghiyev**

Scientific secretary of the Dissertation council

Ph. D. Chem. **Ulviyya Akhmed Mammadova**

Chairman of the scientific seminar

D. Sci. Chem., professor **Akif Shikhan Aliyev**

GENERAL DESCRIPTION OF WORK

Relevance and degree of investigation of the topic. Achievements in science and technology are closely related to the receipt and use of materials with a number of unique functional properties, such as photoelectric, optical, thermoelectric, magnetic, superionic conductivity, superconductivity, topological insulator, and high technologies based on them. The development of modern materials science associated with the search and development of materials with a number of necessary properties and the improvement of the properties of already known compounds. It is not surprising that the world's leading scientific centers conduct ongoing research in these areas.

The rapid development of nanomaterials science, the chemistry of supramolecular compounds, superionic conductors, high-entropy alloys (HEA), etc., the discovery of graphene and topological insulators at the beginning of this century served as a new powerful impulse for research in the field of chemistry and materials science of chalcogenides.

Metal chalcogenides, as well as multicomponent phases based on them, are important functional materials that exhibit the above properties and have found application in a number of technologies. In particular, rare-earth elements (REE) chalcogenides, which have unique magnetic, optical, and thermoelectric properties, resistance to sudden changes in environmental conditions, high thermal stability, etc. occupy a special position among these materials. These materials are characterized by high specific strength, excellent mechanical characteristics at high temperatures, exceptional ductility and fracture toughness at cryogenic temperatures, superparamagnetism, and superconductivity. HEA based on REE can be good thermoelectric materials due to the large Seebeck coefficient and low thermal conductivity.

Thallium is an element with a high density (11.85 g/cm^3) and its incorporation into the crystal lattice of known binary thermoelectrics leads to a decrease in the band gap and thermal conductivity, and as a result, to an increase in the thermoelectric figure of merit of the materials. Therefore, many complex thallium-based chalcogenides are classified as thermoelectrics with anomalously low thermal conductivity.

In recent years, interest has increased in complex thallium chalcogenides as well as in Weyl semimetals and topological insulators. In addition, some of these compounds are characterized by high photoconductivity, which makes them promising for use as detectors of γ- and X-ray radiation.

The unfilled 5d- and 4f- levels of thallium, screen the $6s^2$ outer shell electrons, leading to a significant difference between the energies of the 6s- and 6p- orbitals (the effect of an inert 6s pair). Therefore, unlike other p^1-elements, thallium is characterized not by the highest degree of oxidation, but by the monovalent state. In compounds in the oxidation state +1 thallium resembles alkali metals as regards chemical and crystallographic properties. At the same time, the presence of $6s^2$ electrons gives Tl^+ some specificity; for example, Tl_2X compounds are more fusible than the corresponding group I metal chalcogenides. The polarization effect in Tl^+ leads both to the modification of the crystal structure, which is characteristic of alkali compounds, and to the appearance of structures of a completely different type. At the same time, thallium in compounds can be in the highest oxidation state (for example, Tl_2X_3), as well as in both oxidation states in the same compound. Examples are the chalcogenides TlSe, TlTe, and Tl_5Te_3.

Thallium subtelluride Tl_5Te_3 is a suitable matrix compound for the synthesis of new compounds – structural analogs and multicomponent phases of variable composition. This compound exhibits thermoelectric properties and, due to the peculiarities of the crystal structure, forms a number of ternary anion- and cation-substituted structural analogs, which also exhibit interesting functional properties. It can be assumed that the incorporation of the heavy REE atoms into the crystal structure of Tl_5Te_3 and its structural analogs will lead to an improvement in thermoelectric properties and giving additional properties, for example, magnetic.

The creation and development of physical and chemical foundations for the controlled synthesis of new multicomponent compounds and materials are based on reliable data on phase equilibria and thermodynamic properties of the corresponding systems. Of particular interest are systems in which the formation of structural ana-

logues of known binary and ternary compounds or solid solutions based on them is possible. It is no coincidence that most of the ternary structural analogs of Tl_5Te_3 were found in the study of phase equilibria in the corresponding systems.

An analysis of the literature data shows that before the beginning of our research (2005), phase equilibria in the Tl-Ln-Te ternary systems had not been studied. There were only fragmentary data on the structural and magnetic properties of compounds of the $TlLnX_2$ (X-S, Se, Te) type.

Object and subject of research. Taking into account the above, the object of study was the Tl_2Te-Tl_5Te_3-Tl_4LnTe_3 (Ln-Sm, Dy, Tm), Tl_2Te-Tl_5Te_3-Tl_9LnTe_6 (Ln-Sm, Gd, Tb, Er, Tm), and Tl_2Te-YbTe-Te composition areas of the Tl-Ln-Te ternary systems, as well as Tl_5Te_3-Tl_9LnTe_6-Tl_9BiTe_6 (Ln-Sm, Gd, Tb, Er, Tm), Tl_5Te_3-Tl_9LnTe_6-Tl_9SbTe_6 (Ln-Sm, Gd, Tb), Tl_2Te-Tl_9LnTe_6-Tl_9BiTe_6 (Ln-Sm, Gd, Er), Tl_2Te-Tl_9LnTe_6-Tl_9SbTe_6 (Ln-Sm, Gd), and Tl_4PbTe_3-Tl_9BiTe_6-Tl_9GdTe_6 composition areas of the quaternary and quintuple systems. The subject of the study was the physicochemical and thermodynamic study of these systems.

The purpose and objectives of the study. Considering the above, the purpose of the dissertation is the creation of the physicochemical foundations for the directed synthesis of thallium-REE tellurides and complex phases of variable composition based on them using a comprehensive study of phase equilibria, crystal-chemical and thermodynamic properties of the corresponding systems.

To achieve this goal, the following **specific tasks** were set and solved:

- planning and organization of experiments for a comprehensive study of phase equilibria and thermodynamic properties of ternary and more complex thallium tellurides of REE using a combination of traditional methods of physicochemical analysis (DTA, XRD, MSA, SEM) with EMF measurements of the concentration cells with liquid electrolyte;
- implementation of such comprehensive studies in some Tl-Ln-Te ternary systems; determination of the nature and parameters of

phase equilibria in ternary systems; construction of some polythermal and isothermal sections of phase diagrams, as well as projections of liquidus surfaces.

- synthesis and identification of synthesized new ternary compounds, determination of their homogeneity regions, types, and parameters of the crystal lattice;
- study of some systems based on the identified new ternary compounds and their structural analogs to obtain solid solutions of variable composition.
- study of thermodynamic properties of some binary Ln-Te and ternary Tl-Ln-Te systems by EMF method.

Research Methods. The studies were carried out using the methods of physicochemical analysis, namely, differential thermal analysis (DTA), X-ray diffraction analysis (XRD), scanning electron microscopy (SEM), as well as measurements of the microhardness and EMF of two types of concentration cells relative to the electrodes.

DTA was carried out in evacuated quartz ampoules on NETZSCH 404 F1 Pegasus system, as well as on a multichannel DTA device assembled based on the electronic TC-08 Thermocouple Data Logger. The diffraction patterns of the alloys were recorded on a Bruker D2 Phaser and D8 ADVANCE powder diffractometers using $CuK_{\alpha 1}$ radiation. SEM images were taken on a JEOLJSM-7600F Field Emission Scanning Electron Microscope. The microhardness measurements, as well as the study of the microstructure, were carried out on a PMT-3 microhardness tester and a ME520TA metallographic microscope.

Methods of theoretical research were N.S. Kurnakov's doctrine of phase relations and the mathematical apparatus of thermodynamics of solutions using the method of partial thermodynamic functions.

Provisions submitted for defense:

- ✓ Prediction of the formation of new thallium-REE tellurides of the Tl_9LnTe_6 and Tl_4LnTe_3 types with the Tl_5Te_3 structure and the developed method for the synthesis of these compounds.
- ✓ Complexes of new mutually consistent data on phase equilibria in Tl-Ln-Te ternary systems in the Tl_2Te-Tl_5Te_3-Tl_4LnTe_3 (Ln-Sm, Dy, Tm), Tl_2Te-Tl_5Te_3-Tl_9LnTe_6 (Ln-Sm, Gd, Tb, Er, Tm), and

Tl_2Te-YbTe-Te, composition regions, including various polythermal and isothermal sections, as well as projections of liquidus and solidus surfaces;

- ✓ Obtained patterns of phase equilibria in the Tl_5Te_3-Tl_9LnTe_6-Tl_9BiTe_6 (Ln-Sm, Gd, Tb, Er, Tm), Tl_5Te_3-Tl_9LnTe_6-Tl_9SbTe_6 (Ln-Sm, Gd, Tb), Tl_2Te-Tl_9LnTe_6-Tl_9BiTe_6 (Ln-Sm, Gd, Er), Tl_2Te-Tl_9LnTe_6-Tl_9SbTe_6 (Ln-Sm, Gd), and Tl_4PbTe_3-Tl_9BiTe_6-Tl_9GdTe_6 systems.
- ✓ Results of thermodynamic analysis and 3D visualization of liquidus and solidus surfaces of the Tl_9GdTe_6-Tl_4PbTe_3-Tl_9BiTe_6 system.
- ✓ Crystallographic parameters of the obtained new ternary compounds and phases of variable composition in the above systems.
- ✓ New complexes of fundamental thermodynamic characteristics of binary and ternary REE tellurides in Ln-Te and Tl-Ln-Te (Ln-Gd, Tb, Er, Tm) systems obtained by EMF method.
- ✓ Magnetic properties of some compounds of the Tl_9LnTe_6 type and solid solutions based on them.
- ✓ Revealed regularities of phase formation and phase equilibria in the studied ternary and more complex systems, as well as the thermodynamic properties of the intermediate phases formed in them.

Scientific novelty. The following new results were obtained in the work, which form the scientific basics for the directed synthesis of thallium-REE tellurides and new multicomponent phases based on them:

- ✓ Based on the analysis of the features of the crystal structure of the Tl_5Te_3 and its known ternary structural analogs, the existence of new thallium-REE tellurides of the Tl_9LnTe_6 and Tl_4LnTe_3 types with the specified structure is predicted. A special procedure for the synthesis of these compounds was developed, using which Tl_9LnTe_6 and Tl_4LnTe_3 compounds were obtained in a homogeneous form and identified. It was shown that, unlike other rare earth elements, ytterbium does not form the above mentioned type ternary compounds.
- ✓ By using the methods of physicochemical analysis (DTA, XRD, MSA, measurements of microhardness) and EMF measurements, a set of new mutually consistent data on phase equilibria, crystallographic and thermodynamic properties of Tl-Ln-Te ternary systems

in the thallium tellurides rich composition regions was obtained. A scheme of phase equilibria was obtained in three Tl-Ln-Te ternary systems in the Tl_2Te-Tl_5Te_3-Tl_4LnTe_3 (Ln-Sm, Dy, Tm) range of compositions, three - in the Tl_2Te-Tl_5Te_3-Tl_9LnTe_6 range of compositions (Ln-Sm, Gd, Tb, Er, Tm) and Tl_2Te-YbTe-Te subsystem. The projections of the liquidus and solidus surfaces of the indicated subsystems, various poly- and isothermal sections of their T-x-y diagrams were constructed, the homogeneity regions and the fields of primary phase crystallization, as well as the types and coordinates of non- and monovariant equilibria, were determined.

- ✓ The nature of phase equilibria in the Tl_5Te_3-Tl_9LnTe_6-Tl_9BiTe_6 (Ln-Sm, Gd, Tb, Er, Tm) (I), Tl_5Te_3-Tl_9LnTe_6-Tl_9SbTe_6 (Ln-Sm, Gd, Tb) (II), Tl_2Te-Tl_9LnTe_6-Tl_9BiTe_6 (Ln-Sm, Gd, Er) (III), Tl_2Te-Tl_9LnTe_6-Tl_9SbTe_6 (Ln-Sm, Gd) (IV) and Tl_4PbTe_3-Tl_9BiTe_6-Tl_9GdTe_6 (V) systems were determined. It is shown that systems (I), (II), and (V) are characterized by the formation of unlimited, while systems (III) and (IV) are characterized by the formation of wide regions of substitutional solid solutions with the Tl_5Te_3 structure.
- ✓ Based on the model of regular solutions, the thermodynamic analysis and 3D visualization of the liquidus and solidus surfaces of the Tl_9GdTe_6-Tl_4PbTe_3-Tl_9BiTe_6 system were carried out and a good agreement with the experiment was obtained.
- ✓ Using the EMF method, new sets of mutually consistent data on the fundamental thermodynamic characteristics of binary and ternary REE tellurides in the Ln-Te and Tl-Ln-Te (Ln-Gd, Tb, Er, Tm) systems were obtained.
- ✓ The nature of the magnetic properties of some compounds of the Tl_9LnTe_6 type and solid solutions based on them were determined. It is shown that the investigated compounds are paramagnetic and obey the Curie-Weiss law.

Theoretical and practical significance. The synthesized new thallium-REE tellurides complement the vast class of ternary compounds which are structural analogs of Tl_5Te_3. The obtained complexes of mutually consistent data on phase equilibria in the studied

systems, crystallographic and thermodynamic characteristics of intermediate phases are the physicochemical basis for the development of methods and the choice of optimal modes for the synthesis and growth of monocrystals of new phases with given composition and properties. The revealed new compounds and phases of variable composition are potential functional materials with thermoelectric and magnetic properties, and after detailed studies of physical properties, they can find practical applications.

The above data sets complement the chemistry, thermodynamics, and materials science of complex chalcogenides and can be entered into the appropriate handbooks and electronic data banks. A number of published works containing these results are included in the Web of Sciences and Scopus international databases. According to "Google Scholar Citations", over 440 citations were made to the author's articles on the topic of the dissertation.

Testing and application. The results of the work were reported and discussed at the following scientific conferences:

VII, VIII, XI Международных научных конференциях "Кинетика и механизм кристаллизации. Кристаллизация как форма самоорганизации вещества" (Иваново, Россия, 2010, 2014, 2021); 8th International Conference "Electronic processes in organic and inorganic materials" (Ivano-Frankovsk, Ukraine, 2010); XI international conference on crystal chemistry of intermetallic compounds (Lviv, Ukraine, 2010); VII Международной научно-технической конференции "Современные методы в теоретической и экспериментальной электрохимии" (Плес, Россия, 2015); XIII-XV International Conference on Physics and Technology of thin films and Nanostructures (Ivano-Frankovsk, Ukraine, 2011, 2013, 2015); XIX Менделеевском съезде по общей и прикладной химии (Волгоград, Россия, 2011); Всероссийской конференции "Современные проблемы химической науки и образования" (Чебоксары, Россия, 2012); XII International conference on crystal chemistry of intermetallic compounds (Lviv, Ukraine, 2013); X Международном Курнаковском Совещании по физико-химическому анализу (Самара, Россия, 2013); 1st International

chemistry and chemical engineering conference (Baku, Azerbaijan, 2013); XV научно-технической конференции "Chemical engineering-2014" (Москва, Россия, 2014); 1st International scientific conference of young scientists and specialists "The role of multidisciplinary aproch in soluti of actual problems of fundamental and applied sciences (earth, technical and chemical)" (Baku, Azerbaijan, 2014); International Conference Applied Mineralogy and Advanced materials, AMAM- 2015 (Castellaneta Marina, Italy, 2015); 1st, 2nd International Turkic World Conference on Chemical Sciences and Technologies, (Sarajevo, Bosnia-Herzegovina, 2015; Skopje, Macedonia, 2016); V International conference "HighMatTech" (Kiev, Ukraine, 2015); Всероссийской научной конференции с международным участием «II Байкальский материаловедческий форум», (Улан-Уде, Россия, 2015); Всероссийской конференции "Химия твердого тела и функциональные материалы" (Екатеринбург, Россия, 2016); XI международное Курнаковское совещание по физико-химическому анализу (Воронеж, Россия, 2016); AMEA-nın akad. M. Nağıyev ad. Kataliz və Qeyri-üzvi Kimya İnstitutunun 80 illik yubileyinə həsr o lunmuş elmi konfransı, (Bakı, Azərbaycan, 2016); IX Международная научно-техническая конференция микро- и нанотехнологии в электронике (Нальчик, Россия, 2017); VIII Всероссийской конференции "Физико-химические процессы в конденсированных средах и на межфазных границах- ФАГРАН-2018" (Воронеж, Россия, 2018); II International scientific conference of Young reserchers (Baku, Azerbaijan, 2018); XXII International Conference on Chemical Thermodynamics in Russia" (Saint-Pererburg, Russia, 2019); Ümummilli lider Heydər Əliyevin anadan olmasmm 94-cü ildönümünə həsr olunmuş "Müasir təbiət və iqtisad elmlərinin aktual problemleri" (Gəncə, Azərbaycan, 2019); International conference on actual problems of chemical engineering, dedicate to the 100th Anniversary of the Azerbaijan State Oil and Industry University (Baku, Azerbaijan, 2020); 10th Rostocker International Conference "Thermophysical Properties for Technical Thermodynamics" (Rostock, Germany, 2021); 1st International Congress of Natural Sciences, ICNAS-2021 (Erzurum, Turkey, 2021).

Based on the materials of the dissertation, 70 scientific works were published, including 37 articles in journals included in the High Attestation Commission list. 26 were published articles in international journals indexed in the Web of Sciences and Scopus.

The name of the organization in which the work was carried out. The dissertation was carried out in the "Thermodynamics of functional inorganic compounds" laboratory of the "Functional inorganic materials" department of the Institute of Catalysis and Inorganic Chemistry named after acad. M.Nagiyev of Azerbaijan National Academy of Sciences.

Volume and structure of work. The dissertation consists of an introduction (18.753 characters), five chapters (Chapter I- 67.118, Chapter II-47.956, Chapter III-62.942, Chapter IV-54.124, Chapter V-103.5263), main results and conclusions, a list of references and published works of the author on the topic of the dissertation (499 titles), as well as Appendix. The dissertation is presented on 382 pages, contains 146 figures and 51 tables.

The Appendix presents powder diffraction patterns of some alloys of the studied systems, phase diagrams of the internal polythermal cross sections of the studied ternary systems, initial data of thermodynamic measurements for binary and ternary systems. The Appendix includes 30 figures and 21 tables.

The contribution of the author. The formulation of the goals and objectives of the dissertation, the development of methodological methods for their solution, processing and generalization of the results, as well as a significant part of the results of experimental studies belongs to author.

Acknowledgments. The author expresses gratitude to prof. Imamaddin Amiraslanov (Institute of Physics, ANAS) and Vagif Gasymov (ICIC, ANAS) for providing assistance in conducting X-ray diffraction studies and interpreting their data. I express my special gratitude to my Teacher and scientific consultant, Corresponding Member of the Azerbaijan National Academy of Sciences, professor Mahammad Babanly for his attention, valuable guidance, discussions, and support.

MAIN CONTENT OF THE WORK

In the **introduction,** the relevance of the topic of the dissertation work is justified, the goal, tasks, scientific novelty, the theoretical and practical significance of the results obtained in the dissertation are formulated, a list of testing of the dissertation results are given.

The first chapter briefly describes and critically analyzes the literature data on T-x diagrams in Tl-Te, Ln-Te binary, and Tl-B^V-Te ternary systems (Ln-Sm, Gd, Tb, Dy, Er, Tm, Yb; B^V-Sb, Bi), as well as the physicochemical properties of thallium tellurides and rare earth tellurides (REE) (paragraphs 1.2-1.4). Paragraph 1.5 presents data on the state of knowledge of complex systems composed of thallium-containing REE tellurides and justifies the choice of research objects. A separate paragraph (1.1) is devoted to a review of studies on various functional properties of heavy metal chalcogenides and materials based on them. Based on the analysis of literature data, the objects of research of the dissertation are substantiated.

The second chapter is devoted to the methodological aspects of planning and organizing mutually agreed investigations on phase equilibria and thermodynamic properties of the studied systems. A brief description of the synthesis methods (paragraph 2.1), as well as the research methods used and the corresponding instruments and devices (paragraph 2.2), are presented. Experimental research methods and related instruments and devices are described above (p.6).

Paragraph 2.3 presents and describes in detail the procedure for the synthesis of ternary thallium-REE tellurides and alloys based on them. In particular, it has been shown that the synthesis of ternary compounds of the Tl_9LnTe_6 and Tl_4LnTe_3 types from elementary initial components by the traditional melting method does not lead to homogeneous samples obtained even after long-time thermal annealing. It has been established that REE with thallium forms stable intemetallics, which prevents the formation of ternary compounds. The use of REE tellurides and thallium tellurides does not lead to obtain of homogeneous samples as well as. Considering the above, a special procedure was developed for the synthesis of ternary compounds: instead of metallic thallium, stoichiometric amounts of thallium tellu-

rides, as well as elemental REE and tellurium, were used. In addition, it has been established that to obtain homogeneous samples after alloying, the long-term annealing (about 1000 h) of cast alloys ground into powder and pressed into pellets is necessary.

During the syntheses, elementary components of a high degree of purity from the German company Alfa Aesar were used (tellurium, CAS № 13494-80-9; thallium 7440-28-0; stibium-7440-36-0; bismuth-7440-69-9; lead-7439-92-1; samarium-7440-19-9; gadolinium-7440-54-2; therbium-7440-27-9; dysprosium - 7429-91-6; erbium-7440-52-0; thulium-7440-30-4; itterbium-7440-64-4).

Alloys of the studied systems were prepared from preliminarily synthesized and identified binary and ternary compounds in quartz ampoules evacuated to ~10^{-2} Pa. To prevent the interaction of lanthanides with quartz walls at high temperatures, the synthesis was carried out in graphitized ampoules. Graphitization was carried out by the decomposition of toluene. Specific synthesis conditions are given in the dissertation.

The third chapter presents the results of an experimental study of the phase relations in the Tl-Ln-Te ternary systems in the composition regions Tl_2Te-Tl_5Te_3-Tl_9LnTe_6 (Ln-Sm, Gd, Tb, Er, Tm) and Tl_2Te-Tl_5Te_3-Tl_4LnTe_3 (Ln- Sm, Dy, Tm), as well as Tl_2Te-YbTe-Te. As examples, some data for the Tl_2Te-Tl_5Te_3-Tl_9SmTe_6 и Tl_2Te-Tl_5Te_3-Tl_4DyTe_3 and Tl_2Te-YbTe-Te systems are given below.

The Tl_2Te-Tl_5Te_3-Tl_9SmTe_6 system

Section Tl_2Te-Tl_9SmTe_6 (Fig.1) of this system is non-quasi-binary due to the incongruent melting of the Tl_9SmTe_6 compound and is characterized by the formation of a wide range of solid solutions (δ-phase) with the Tl_5Te_3 structure. Liquidus consists of primary crystallization curves of the $TlSmTe_2$ compound, as well as α- and δ- phases based on Tl_2Te and Tl_9SmTe_6, respectively. The horizontal lines at 703 and 755 K correspond to the peritectic equilibria $L+\delta \leftrightarrow \alpha$ and $L+TlSmTe_2 \leftrightarrow \delta$.

The microhardness values of the samples within the homogeneity regions of the α- and δ- phases increase somewhat, and in the two-phase region α+δ remain constant regardless of the composition of the alloy (Fig. 1b).

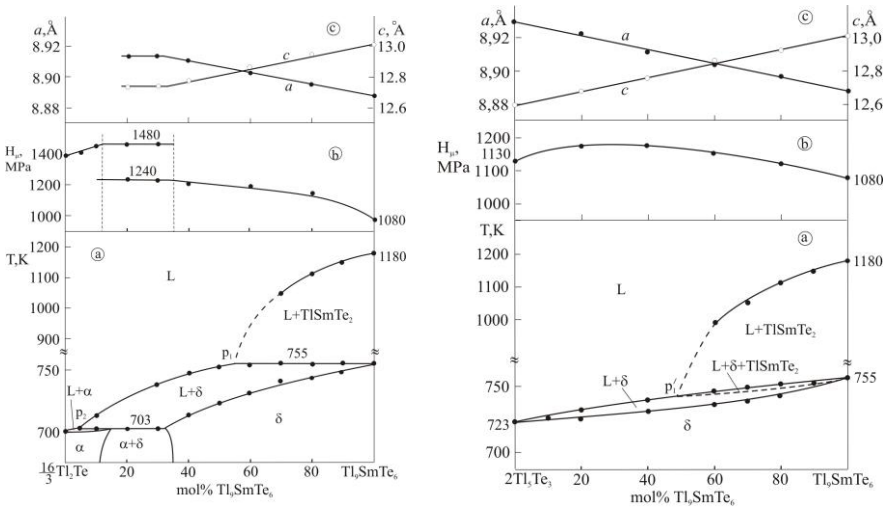

Picture 1. Phase diagrams of the Tl_2Te-Tl_9SmTe_6 and Tl_5Te_3-Tl_9SmTe_6 systems.

The Tl_5Te_3-Tl_9SmTe_6 system (Fig. 1) is also non-quasi-binary and is characterized by the formation of a continuous series of solid solutions (δ-phase). In the 0-50 mol% Tl_9SmTe_6 concentration interval, the crystals of δ-solid solutions primarily precipitate from the liquid. In the region with a higher Tl_9SmTe_6 concentration, the $TlSmTe_2$ compound first crystallizes. As a result of the L+$TlSmTe_2$↔δ monovariant peritectic reaction in this region below a temperature of 755 K, a three-phase region L+$TlSmTe_2$+δ should form. However, this field was not experimentally fixed due to the narrow temperature interval and is marked by a dashed line.

The concentration dependence of the microhardness of the samples is characterized by a curve passing through a soft maximum, which is typical for systems with continuous solid solutions (Fig. 1b).

The results of XRD (Fig.2) confirmed the phase diagrams (Fig.1) of the above systems. In the Tl_2Te-Tl_9SmTe_6 system (diffractograms 1-4), the alloys with compositions ≥30 mol% Tl_9SmTe_6 are single-phase and have diffraction patterns of the Tl_5Te_3 type (3), and the alloy with the composition 25 mol% Tl_9SmTe_6 (2) is two-phase and,

along with the reflections of δ-phase, contains weak reflections of the α-phase. In the Tl_5Te_3-Tl_9SmTe_6 system (diffractograms 4-6), the initial compounds and the alloy of composition 50 mol% Tl_9SmTe_6 have similar diffraction patterns with a slight shift of reflections. The dependences of the crystal lattice parameters of the alloys of the Tl_5Te_3-Tl_9SmTe_6 system obey Vegard's rule (Fig. 1c).

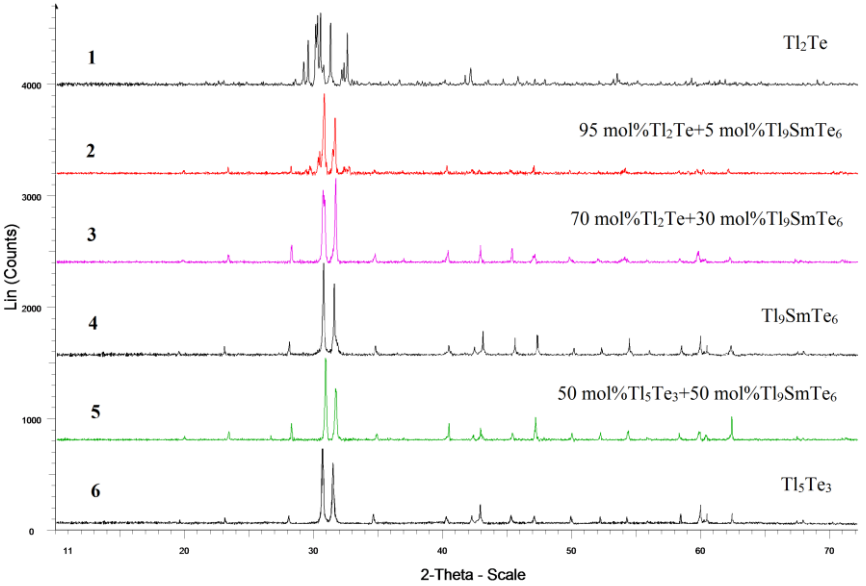

Fig.2. Powder diffraction patterns of alloys of the Tl_2Te-Tl_9SmTe_6 (№№1-4) and Tl_5Te_3-Tl_9SmTe_6 (№№4-6) systems

Liquidus and solidus surfaces projections of the Tl_2Te-Tl_5Te_3-Tl_9SmTe_6 system (Fig.3). Liquidus consists of three fields of the primary crystallization of the $TlSmTe_2$ compound, as well as α-, δ-phases. Curves p_2e and p_1p_1' separating these fields correspond to $L+\delta\leftrightarrow\alpha$ and $L+TlSmTe_2\leftrightarrow\delta$ monovariant peritectic equilibria. The surfaces of the solidus correspond to two surfaces, showing the completion of crystallization of the α- and δ-phases.

The dissertation presents and discusses a number of polythermal sections of the phase diagram of the Tl_2Te-Tl_5Te_3-Tl_9SmTe_6 system. *The diagram of solid-phase equilibria at 300 K of the Tl_2Te-Tl_5Te_3-Tl_9SmTe_6*

system consists of three phase areas. The largest part (more than 90%) of the area of the concentration triangle is occupied by the region of homogeneity of δ-solid solutions with a perovskite-like structure

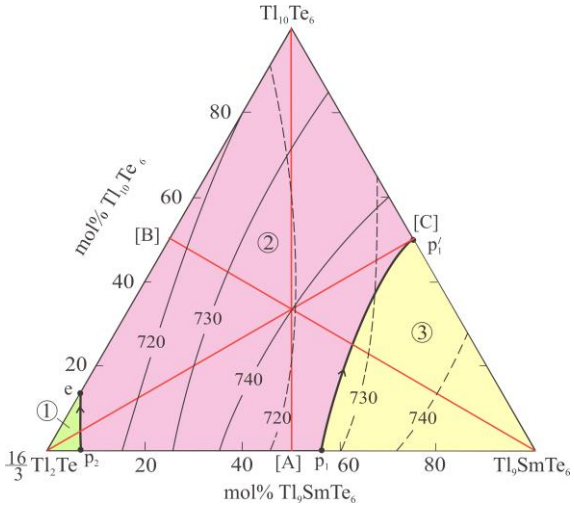

Figure 3. Liquidus and solidus surfaces projection (dashed lines) of the Tl_2Te-Tl_5Te_3-Tl_9SmTe_6 system. Fields of primary crystallization of phases: 1-α; 2-δ; 3-$TlSmTe_2$. Red dashed lines - studied polythermal sections.

Isothermal sections at 720, 730, and 740 K of the phase diagram of the Tl_2Te-Tl_5Te_3-Tl_9SmTe_6 system consist of three fields and clearly show the directions of the connodes in two-phase regions. The directions of connodes change with temperature, which is typical for non-quasi-binary systems.

Phase equilibria in the Tl_2Te-Tl_5Te_3-Tl_4DyTe_3 system

The isothermal section of the phase diagram at 300 K

As can be seen, along the Tl_5Te_3- Tl_4DyTe_3 section (Fig. 4), the initial compounds and intermediate alloys have the same diffraction pattern with a certain shift of the reflection lines, which indicates the formation of a continuous series of solid solutions. Along the Tl_2Te-Tl_9DyTe_6 and Tl_2Te-Tl_4DyTe_3 sections, alloys containing more than 30 mol% Tl_9DyTe_6 are single-phase, and alloys with compositions of 20 mol% Tl_9DyTe_6(Tl_4DyTe_3) consist of α+δ two-phase mixture.

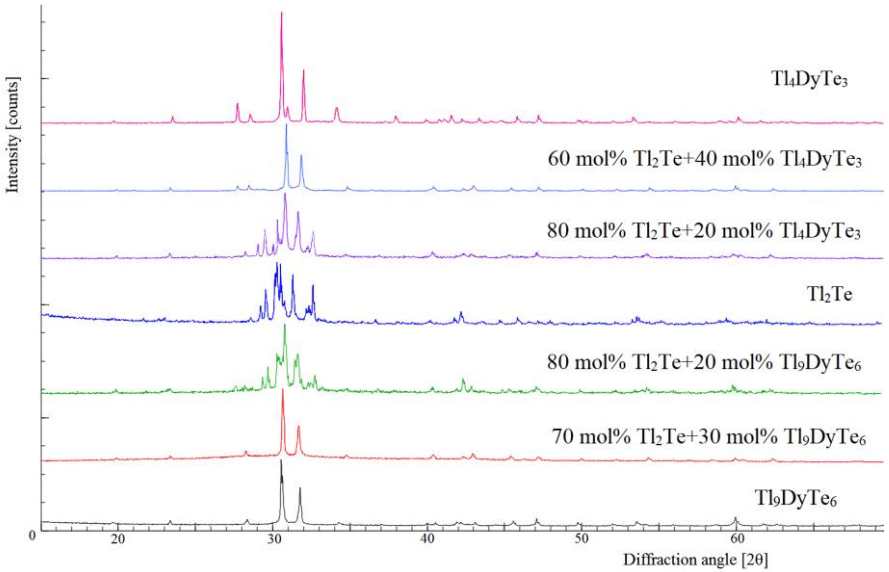

Figure 4 Powder diffraction patterns of alloys along the Tl_2Te-Tl_9DyTe_6 and Tl_2Te-Tl_4DyTe_3 sections of the Tl_2Te-Tl_5Te_3-Tl_4DyTe_3 system.

Based on the XRD data of boundary systems and a number of alloys within the concentration region, a diagram of solid-phase equilibria at 300 K was constructed (Fig. 5). As can be seen, α, δ and α+δ phase regions are formed in the Tl_2Te-Tl_5Te_3-Tl_4DyTe_3 subsystem. A continuous series of δ-solid solutions in the Tl_5Te_3-Tl_4DyTe_3 boundary system penetrates deep into the concentration triangle and covers over 90% of its area. Based on Tl_2Te, a narrow region of homogeneity (α-phase) is formed. These single-phase regions are separated by α+δ two-phase field, in which the compositions of coexisting phases are on the plane of the elementary triangle of the Tl_2Te-Tl_5Te_3-Tl_4DyTe_3 system. Thus, the studied concentration region of the Tl-Dy-Te system below the solidus is an independent subsystem.

*Liquidus and solidus surfaces projections***.** The liquidus of the Tl_2Te-Tl_5Te_3-Tl_4DyTe_3 system (Fig. 6) corresponds to four fields of primary crystallization of α-, δ-phases, as well as $TlDyTe_2$ and DyTe

compounds that exist outside the considered concentration region. These fields are delimited by a number of curves of monovariant equilibria and nonvariant points. The types and temperatures of these equilibria are given in Table 1.

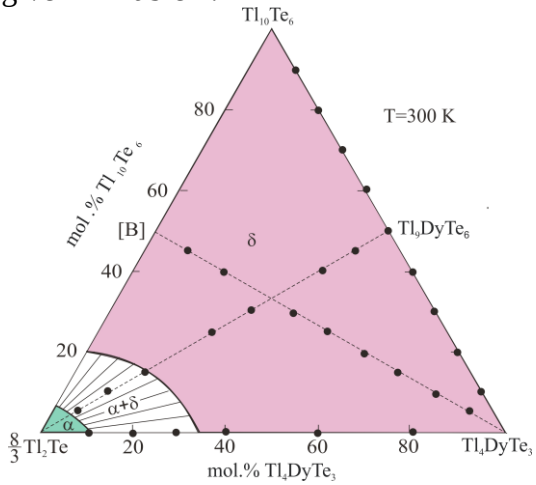

Figure 5. The isothermal section of the phase diagram of the Tl_2Te-Tl_5Te_3-Tl_4DyTe_3 system at 300K. Dashed lines are the studied internal sections. The points - are the compositions of the studied alloys.

The KU curve delimiting the liquidus surfaces of $TlDyTe_2$ and DyTe is a fragment of the eutectic curve, which starts from the point of nonvariant transitional equilibrium $L+Dy_2Te_3 \leftrightarrow TlDyTe_2+DyTe$ which is beyond the concentration triangle. The intersection of the KU curve with the peritectic curve p_1U leads to the establishment of an nonvariant transitional equilibrium U in the system (Fig. 6., Table 1). Another peritectic curve delimits the liquidus surfaces of $TlDyTe_2$ and the δ-phase. Fig.6 reflects the p_3M fragment of this curve, which continues beyond the Tl_2Te-Tl_5Te_3-Tl_4DyTe concentration triangle.

Thus, unlike the diagram of solid-phase equilibria (Fig. 5), the projection of the liquidus and solidus surfaces of the phase diagram of the Tl-Dy-Te system in the considered concentration region (Fig. 6) is not an independent subsystem, since the $TlDyTe_2$ and DyTe solid phases involved in heterogeneous equilibria (Table 1) are outside this area.

Table 1

Non- and monovariant equilibria in the Tl_2Te-Tl_5Te_3-Tl_4DyTe_3 system.

Point or curve on Fig.6	Equilibria	T, K
p_1	$L+DyTe \leftrightarrow Tl_4DyTe_3$	767
p_2	$L+\delta \leftrightarrow \alpha$	706
p_3	$L+TlDyTe_2 \leftrightarrow Tl_9DyTe_6$	743
p_4	$L+\delta \leftrightarrow \alpha$	703
e	$L \leftrightarrow \alpha+\delta$	693
U	$L+DyTe \leftrightarrow TlDyTe_2+\delta$	750
KU	$L \leftrightarrow DyTe+TlDyTe_2$	1180-750
p_2p_4; p_4e	$L+\delta \leftrightarrow \alpha$	706-703; 703-693
p_1U	$L+DyTe \leftrightarrow \delta$	767-750
Up_3; p_3M	$L+TlDyTe_2 \leftrightarrow \delta$	750-743; 743-735

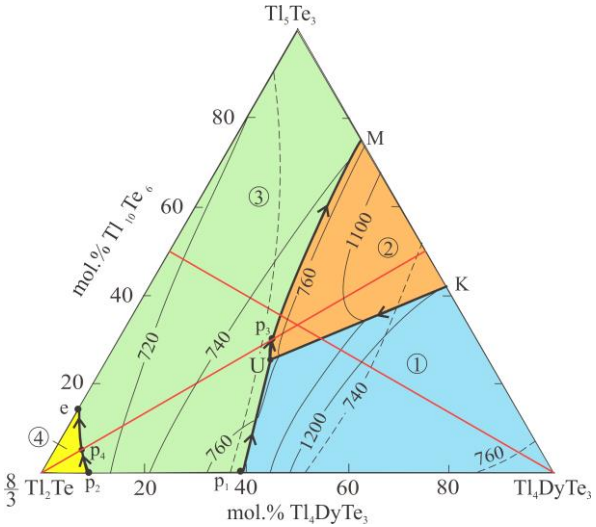

Figure 6. Projections of the liquidus and solidus surfaces of the Tl_2Te-Tl_5Te_3-Tl_4DyTe_3 system. Fields of primary crystallization: 1- DyTe; 2-$TlDyTe_2$; 3-δ; 4-α. Red lines –are studied polythermal sections.

Section Tl_5Te_3-Tl_4DyTe_3 (Fig. 7). This section is interesting due to formation of a continuous series of solid solutions (δ) with the Tl_5Te_3

structure and the fact that the Tl_9DyTe_6 ternary compound, the second structural analog of Tl_5Te_3, is within the homogeneity region of the δ-phase. As can be seen from Fig. 7, the liquidus consists of the curves of primary crystallization of the δ-phase, $TlDyTe_2$, and DyTe. The DTA curves do not reveal any thermal effects corresponding to the liquidus of DyTe. The L+DyTe region is delimited by us with a dashed line according to the general T-x-y diagram. The dashed line also marks the three-phase region L+ Dy-Te+ $TlDyTe_2$, which separates two two-phase regions.

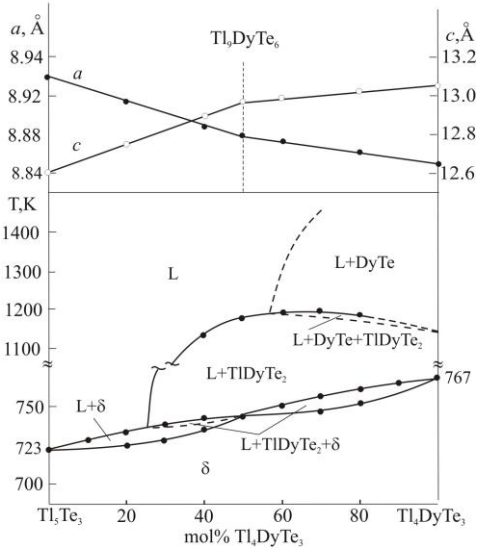

Figure 7. Tl_5Te_3-Tl_4DyTe_3 polythermal section.

An analysis of the DTA curves of the annealed alloys also showed that unlike other compositions of the δ-phase melting in the temperature range, the alloy of composition 50 mol % Tl_4DyTe_3 (Tl_9DyTe_6 composition) melts with decomposition at a constant temperature (767 K). On the other hand, on the graph of the concentration dependence of the parameters of the tetragonal lattice of the δ-phase, breakpoints are distinctly fixed for a given composition.

In the 0÷50 mol% Tl_4DyTe_3 range of compositions, a sharp decrease in lattice parameter *a* and an increase in parameter *c* are ob-

served. This is apparently related to the strengthening of the chemical bond between the Dy^{3+} atoms in the centers of the octahedra and Te(2). In the >50 mol % Tl_4DyTe_3 region of compositions, a less decrease in lattice parameter *a* and an increase in parameter *c* are observed. This can be explained by the fact that in the indicated range of compositions, simultaneously with the replacement of the second half of the Tl(2) atoms with the oxidation state +1 by dysprosium, the transition of Dy^{3+} ions to Dy^{2+} occurs which has a slightly larger crystallographic radius. The combination of two competing processes leads to fewer changes in the lattice parameters than in the range of compositions 0÷50 mol % Tl_4DyTe_3.

The results of XRD analysis showed that the Tl_9DyTe_6 and Tl_4DyTe_3 compositions of the δ-phase differ from others: all atoms in them, including Dy, have strictly defined crystallographic positions, which is typical for a chemical compound. In addition, in Tl_9DyTe_6, dysprosium has an oxidation state of +3, and in Tl_4DyTe_3 is +2.

The work presents and discusses some polythermal sections: Tl_2Te-Tl_4DyTe_3, Tl_2Te-Tl_9DyTe_6, Tl_4DyTe_3-[B] ([B] is an alloy of 50 mol% Tl_5Te_3 composition of the Tl_2Te-Tl_5Te_3 boundary system).

In the third chapter, the results of the study of the physicochemical interaction in the Tl_2Te-Tl_5Te_3-Tl_9LnTe_6 (Ln-Gd, Tb, Er, Tm) и Tl_2Te-Tl_5Te_3-Tl_4LnTe_3 (Ln-Sm, Tm) systems, including projections of liquidus and solidus surfaces, some poly- and isothermal sections of phase diagrams, are presented and discussed in detail.

Somewhat different nature of the physico-chemical interaction is observed in the Tl_2Te-YbTe-Te system (Fig.8, 9). The phase diagrams of the YbTe-Tl_2Te (Tl_5Te_3, TlTe, Tl_2Te_3) systems are described in detail in the dissertation. The YbTe-Tl_5Te_3 and YbTe-Tl_2Te sections are quasi-binary, and the TlTe-YbTe and Tl_2Te_3-YbTe sections are non-quasi-binary due to the incongruent melting of the corresponding thallium tellurides but are stable below the solidus. According to the obtained experimental data, the alloys of the compositions [$TlYbTe_2$], [Tl_9YbTe_6], and [Tl_4YbTe_3] are two-phase. Their powder diffraction patterns consist of a set of reflection lines of the initial binary tellurides.

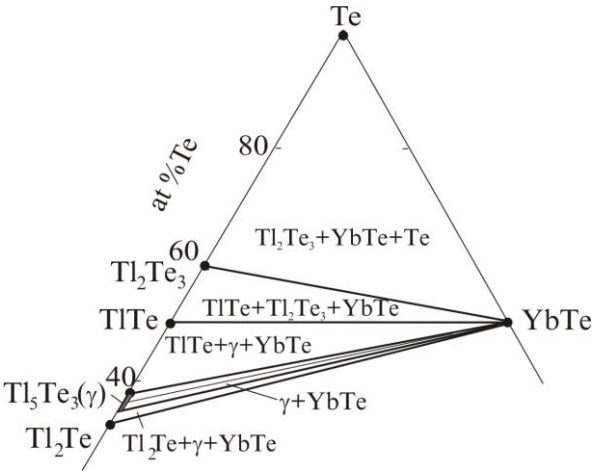

Figure 8. Solid-phase equilibria diagram of the Tl_2Te-YbTe-Te system.

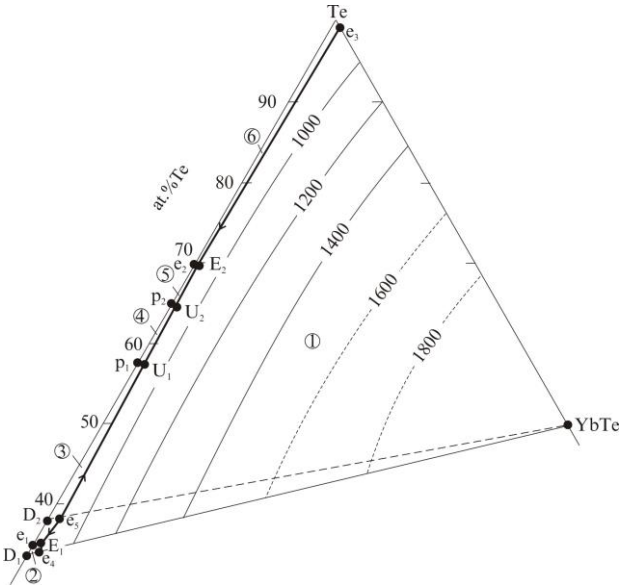

Figure 9. Projection of the liquidus surface of the Tl_2Te-YbTe-Te system. Fields of primary crystallization: 1-YbTe; 2-Tl_2Te; 3-γ; 4- TlTe; 5-Tl_2Te_3; 6-Te. The dashed line - is the Tl_5Te_3-YbTe quasi-binary section

It can be seen from the solid-phase equilibria diagram (Fig. 8), all thallium tellurides form stable connodes with YbTe.

The liquidus surface of the system (Fig. 9) consists of 6 fields corresponding to the primary crystallization of YbTe, Tl_2Te, γ, TlTe, Tl_2Te_3, and Te. The largest area is occupied by the field of primary crystallization of the thermodynamically and thermally most stable YbTe compound. The somewhat different nature of the physicochemical interaction in the Tl-Yb-Te ternary system from other ternary systems of the Tl-Ln-Te type can be explained by the stability of the $4f^{14}5d^{0}6s^{2}$ electronic configuration of the ytterbium atom. The fully-filled outer $4f^{14}$ orbit practically does not take part in the formation of chemical bonds. Therefore, ytterbium has an oxidation state of +2 rather than +3, which is characteristic of lanthanides in compounds of the Tl_9LnTe_6 and $TlLnTe_2$.

At the end of Chapter III, the features of the crystal structure of Tl_5Te_3 and its ternary structural analogs are considered.The main structural elements of the Tl_5Te_3 crystal lattice (Fig. 10) are tellurium octahedra in which the tellurium atoms have two different positions: some of them (Te1) are located in two opposite vertices of the octahedra along *c* axis, and the others (Te2) occupy the remaining positions. The thallium atoms in their positions in the crystal lattice can also be divided into two types: some cations Tl(1) are located in equivalent 16-fold positions, and the others Tl(2) are in fourfold positions. The chemical composition of the unit cell is $Tl_{16}Tl_4Te_8Te_4$. Taking into account the electroneutrality condition, we can assume that Tl^{+} and Tl^{3+} ions alternate in the fourfold positions, and the unit cell may be presented as $Tl_{16}[(Tl^{1+}_{0,5}Tl^{3+}_{0,5})Te_3]_4$. The octahedra share vertices to form a Tl_4Te_{12} or $(TlTe_3)_4$ framework (Fig. 10a). Thallium prisms are formed around octahedra, and thallium antiprisms are formed around anions in octahedral vertices to link octahedra along axis *c*. These structural elements are linked to one another to build a Tl_5Te_3-type structure with $Tl_{16}(TlTe_3)_4$ unit cells (Fig. 10b).

Due to the above structural features, Tl_5Te_3 forms a series of cationsubstituted derivatives: Tl_9BTe_6 (B = Sb, Bi, In, Au, or lanthanide) compounds and Tl_4ATe_3 (A =Sn, Pb, Cu, Mo, or Nd) compounds.

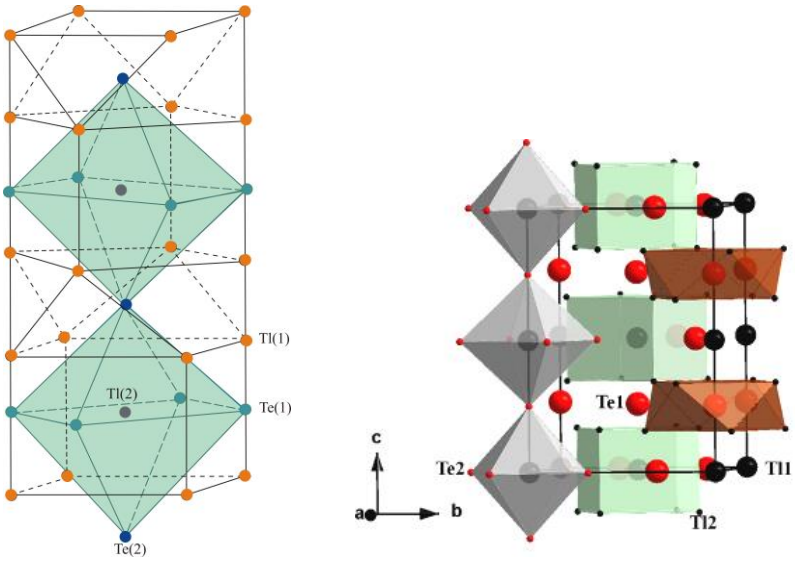

a) b)

Figure 10. Crystal structure of Tl_5Te_3. Main structural element (a), projection onto plane *b, c* (b).

Tl_4ATe_3 compounds are formed when all thallium atoms that center the octahedral (Tl2) are substituted by A^{2+} ions. The substitution of one-half Tl atoms residing in octahedral voids (Tl2) by B^{3+} ions leads to the formation of Tl_9BTe_6 compounds. In other words, in the octahedron in 4-fold positions, the atoms of thallium and the trivalent element alternate alternately.

It is known that lanthanides exhibit oxidation states +2 and +3. The difference between the crystallographic radii of the Ln^{2+}, Ln^{3+}, and Tl^{3+} ions does not exceed 10–12%. With this in mind, we predicted and successfully synthesized thallium-REE tellurides of the Tl_9LnTe_6 and Tl_4LnTe_3 types. It is shown that, unlike other lanthanides, ytterbium does not form ternary compounds of the Tl_9LnTe_6 and Tl_4LnTe_3 types.

The results of our studies showed that all synthesized compounds of the Tl_9LnTe_6 and Tl_4LnTe_3 types have wide regions of homogeneity

(δ-phase), which cover a significant part of the concentration triangles. We have found also that the δ-phases with stoichiometric compositions Tl_9LnTe_6 and Tl_4LnTe_3 differ from its other compositions: in Tl_9LnTe_6 and Tl_4LnTe_3, all atoms, including REE, have strictly defined crystallographic positions, which is typical for a chemical compound. In addition, in Tl_9LnTe_6 compounds, the REE atom exhibits an oxidation state of +3, while in Tl_4LnTe_3 compounds an oxidation state of the REE is +2.

The Figures 11 and 12 show the dependences of the crystal lattice parameters of the Tl_9LnTe_6 and Tl_4LnTe_3 compounds on the serial number of the lanthanide.

Comparison of the crystallographic data of ternary compounds with each other and with the Tl_5Te_3 compound shows that:

1. In compounds of both types, with an increase in the serial number of the lanthanide, a regular decrease in the lattice parameters of the crystal lattice occurs (Fig. 11, 12). This can be explained by lanthanide contraction.

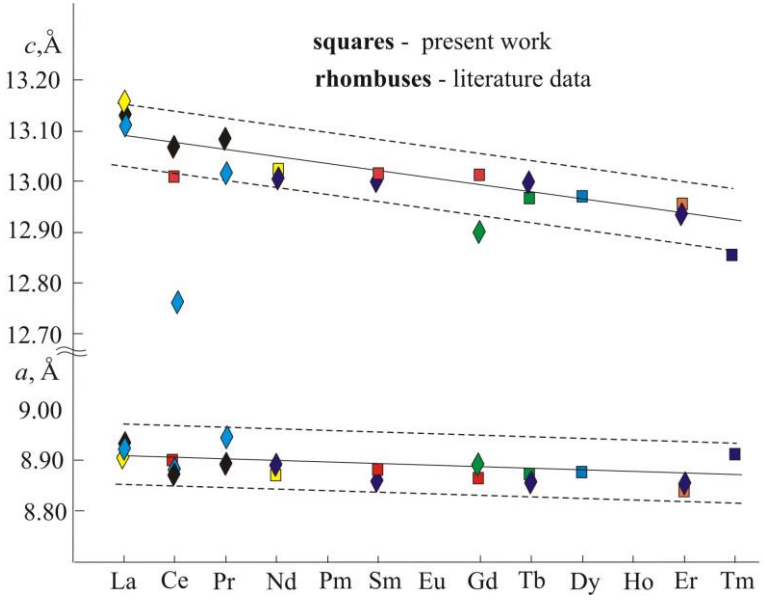

Figure 11. Dependences of the crystal lattice parameters of Tl_9LnTe_6 compounds on the lanthanide serial number.

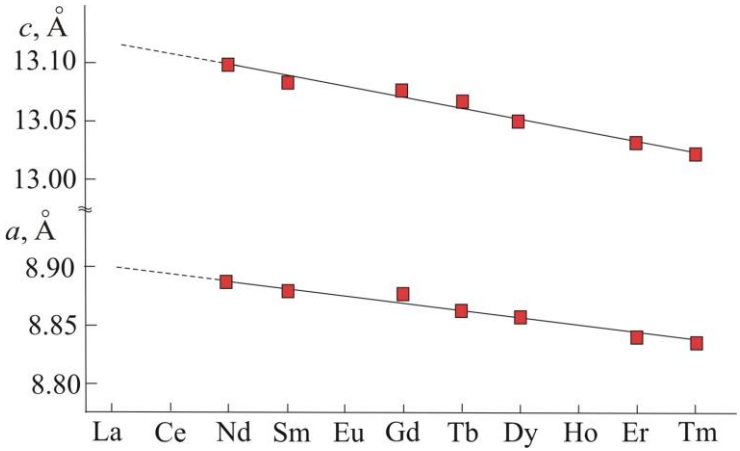

Figure 12. Dependences of the crystal lattice parameters of Tl_4LnTe_3 compounds on the lanthanide serial number.

2. Compared with the corresponding lattice parameters of Tl_5Te_3 in ternary compounds, a decrease in *a* parameter and an increase in *c* parameter are observed (Table 2). In our opinion, this is due to the fact that when thallium (Tl2) atoms in the centers of octahedra are replaced by REE atoms, their chemical bonding with Te(1) atoms is significantly enhanced. This leads to a decrease in the bond length and deformation of the octahedra, which is accompanied by the above changes in the parameters.

In the fourth chapter, to obtain intermediate substitutional solid solutions crystallizing in the Tl_5Te_3 structure, the results of a study of phase equilibria in the Tl-Ln-Bi(Sb)-Te systems (paragraphs 4.1-4.3) and Tl-Pb-Bi-Ln-Te along some concentration planes (paragraph 4.4) are showed. Paragraph 4.5 presents the results of 3D- modeling of the Tl_4PbTe_3-Tl_9BiTe_6- Tl_9GdTe_6 system.

Tl_5Te_3-Tl_9GdTe_6-Tl_9BiTe_6 system

The Tl_9GdTe_6-Tl_9BiTe_6 section (Fig. 13) is characterized by the formation of unlimited solid solutions (δ-phase) with the Tl_5Te_3 structure.

The concentration dependence of the microhardness of the samples is characterized by a curve passing through a gentle maximum, which is typical for systems with unlimited solid solutions (Fig. 13b).

Table 2

Crystallographic parameters of Tl_5Te_3 and synthesized thallium-REE tellurides

Phase	Tetragonal lattice parameters, Å		
	a	*c*	*Z*
Tl_5Te_3	8.930	12.589	4
Tl_9LaTe_6	8.9220(4)	13.156(1)	2
Tl_9CeTe_6	8.9002(9)	13.015(12)	2
Tl_9NdTe_6	8.8976(8)	13.010(11)	2
Tl_9SmTe_6	8.8881(8)	13.013(12)	2
Tl_9GdTe_6	8.8707(9)	13.021(10)	2
Tl_9TbTe_6	8.8711(8)	12.973(12)	2
Tl_9ErTe_6	8.8501(8)	12.952(11)	2
Tl_9TmTe_6	8.8910(9)	12.847(12)	2
Tl_4NdTe_3	8.8885(7)	13.095(12)	4
Tl_4SmTe_3	8.8752(6)	13.078(11)	4
Tl_4GdTe_3	8.8766(7)	13.075(13)	4
Tl_4TbTe_3	8.8652(7)	13.065(12)	4
Tl_4DyTe_3	8.8588(7)	13.052(16)	4
Tl_4ErTe_3	8.8421(6)	13.033(11)	4
Tl_4TmTe_3	8.8354(7)	13.015(15)	4

The XRD data confirmed the phase diagram also. The parameters of crystal lattices, calculated using the TOPAS 3.0 program, obey Vegard's law (Fig. 13, c).

The projection of the liquidus surface (Fig.14) consists of the fields of primary crystallization of the $TlGdTe_2$ compound and δ-solid solutions. These fields are separated by the *ab* curve corresponding to the monovariant peritectic equilibrium $L + TlGdTe_2 \leftrightarrow \delta$. The solidus is represented by one surface, corresponding to the completion of the crystallization of the δ-phase.

The work considers a number of internal polythermal sections.

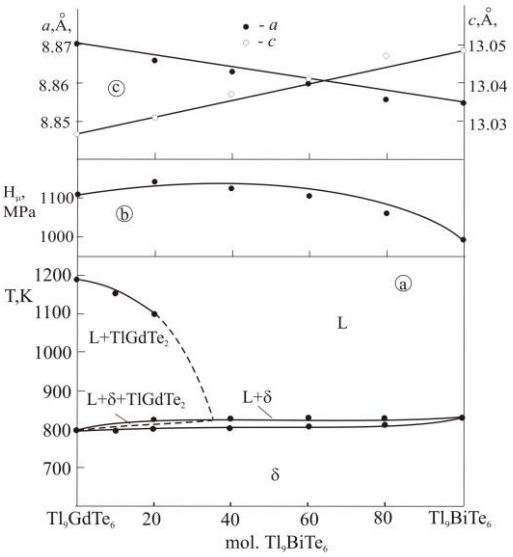

Figure 13. Phase diagram (a), dependences of microhardness (b), and crystal lattice parameters (c) of alloys of the Tl_9GdTe_6-Tl_9BiTe_6 system.

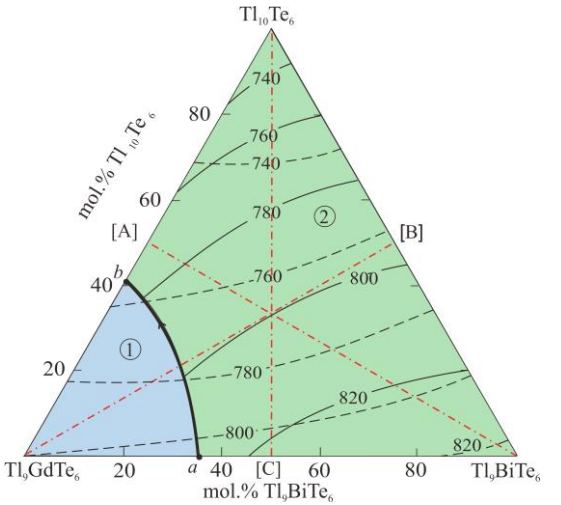

Figure 14. Projection of the liquidus surface of the Tl_5Te_3-Tl_9GdTe_6-Tl_9BiTe_6 system. Fields of primary phase crystallization: 1- TlGdTe2; 2-δ. The studied internal sections are indicated by red dotted lines.

The isothermal sections of the phase diagram at 740, 760, and 820 K (Fig.15) clearly show the scheme of phase equilibria at these temperatures. The cross-sections consist of single-phase fields L and δ separated by L+δ two-phase region. It should be noted that the indicated isothermal sections and polythermal sections show that the directions of connodes in the two-phase region L+δ deviate from the T–x plane, i.e. change with temperature, which is typical for quasi-ternary systems.

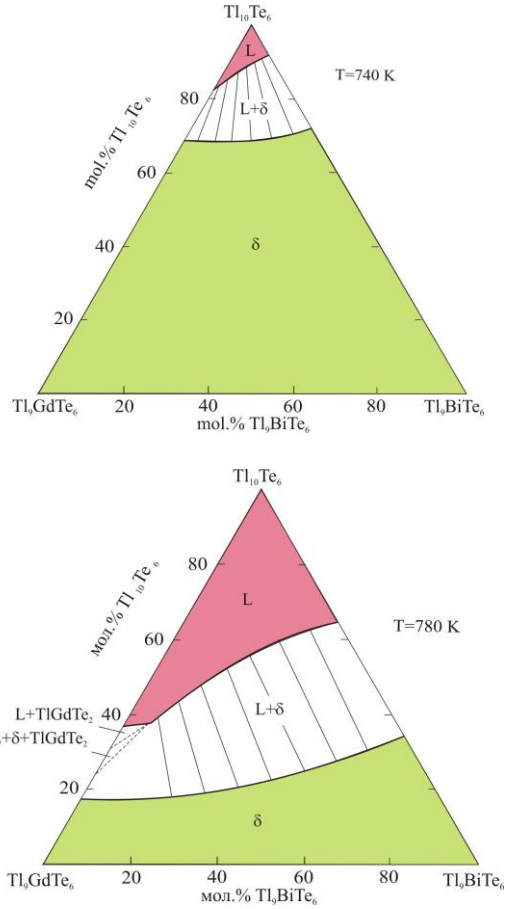

Fug.15. Isothermal sections of the phase diagram of the Tl_5Te_3-Tl_9GdTe_6-Tl_9BiTe_6 system at 780 and 800 K.

The isothermal sections of the phase diagram of the Tl_5Te_3-Tl_9GdTe_6-Tl_9BiTe_6 system at 780 and 800 K (Fig.15) have a somewhat different pattern of phase relations at these temperaturse. They consist of five fields. In alloys containing <60 mol.% Tl_9GdTe_6 in the L + δ two-phase region, the directions of the connodes in the plane of the studied composition. Therefore, this part of the section can be considered stable. In the L + $TlGdTe_2$ two-phase region, as well as in the region L+δ, rich in Tl_9GdTe_6, the directions of the connodes go beyond the planes of this composition. The narrow three-phase region L+$TlGdTe_2$+δ, which should be between the two-phase regions indicated above, is not fixed on the heating curves.

A similar scheme of phase equilibria is also observed in the Tl_5Te_3-Tl_9LnTe_6-Tl_9BiTe_6 (Ln-Sm, Dy, Tb, Er, Tm), as well as Tl_5Te_3-Tl_9LnTe_6-Tl_9SbTe_6 (Ln-Sm, Gd, Tb) systems.

The dissertation also considers in detail the systems of types Tl_2Te-Tl_9LnTe_6-Tl_9BiTe_6 (Ln-Sm, Gd, Er) and Tl_2Te-Tl_9LnTe_6-Tl_9SbTe_6 (Ln-Sm, Gd). Boundary phase diagrams, projections of liquidus and solidus surfaces, a number of poly- and isothermal sections are constructed. The nature of the physicochemical interaction in them is similar to the Tl_2Te-Tl_5Te_3-Tl_9LnTe_6 type ternary systems. It has been established that the systems are characterized by the formation of wide fields of solid solutions with the structure Tl_5Te_3 (δ-phase), occupying most part of the concentration triangles.

The Tl_9GdTe_6-$2Tl_4PbTe_3$-Tl_9BiTe_6 system is characterized by the formation of unlimited solid solutions with the Tl_5Te_3 structure.

3D modeling of the Tl_9GdTe_6-$2Tl_4PbTe_3$-Tl_9BiTe_6 system. Based on the phase diagrams of the boundary binary systems and a limited number of DTA data for samples of the ternary system, the analytical models of T-x phase diagrams of the Tl_9GdTe_6-Tl_4PbTe_3 and Tl_9GdTe_6-Tl_9BiTe_6 boundary systems were obtained, the boundaries of the liquidus surface and solidus of solid solutions and the $TlGdTe_2$ compound were determined. Based on the model of regular solutions of nonmolecular compounds, the thermodynamic functions of mixing the solid solutions are determined. It is shown that solid solutions based on the ternary compounds Tl_9GdTe_6, Tl_4PbTe_3, and

Tl_9BiTe_6 are thermodynamically stable over the entire range of concentrations and temperatures.

The fifth chapter presents the results of a thermodynamic study of the Ln-Te and Tl-Ln-Te (Ln-Gd, Tb, Er, Tm) systems by the EMF method with a liquid electrolyte.

Paragraphs 5.1-5.6 provide an overview of experimental methods for studying thermodynamic properties, briefly describe the basics of the EMF method, note its most widely used modifications, methods for assembling concentration cells and EMF measurements, as well as processing the results of EMF measurements and presenting thermodynamic data.

For the investigations, the concentration cells

(-) Ln (s.) | glycerol+KCl+ $LnCl_3$ | (Ln in alloy) (s. (+) (1)

(-) LnTe(s.) | glycerol+KCl+ $LnCl_3$ | (Ln in alloy) (s.) (+) (2)

were assembled and measured their EMF in the 300-450 K temperature range. The upper limit of the temperature range of EMF measurements was chosen so that the phase composition remained unchanged during the experiment.

Cells of type (1) were used for the study of alloys from the LnTe+Ln_2Te_3 regions, while cells of type (2) were used to study alloys from other phase regions of Ln-Te systems and for the study of Tl-Ln-Te ternary systems.

In cells of both types, a glycerol solution of KCl with the addition of $LnCl_3$ was used as an electrolyte. Before the experiments, glycerol was degassed by pumping under a vacuum at a temperature of ~450 K. Anhydrous, chemically pure KCl and $LnCl_3$ salts were used. In both cells, equilibrium alloys from the studied phase regions were used as right electrodes.

Methods for preparing electrodes and electrolyte, as well as assembling an electrochemical cell, are described in detail in the dissertation. Assembled electrochemical cell vacuumized, filled with argon, and placed in a cylindrical furnace. All contacts and leads of the cell were kept at the same temperature.

The left electrodes were prepared by attaching Ln (LnTe) to a molybdenum wire, and the anodes were prepared by pressing powder alloys onto the wire in the form of cylindrical pellets weighing ~0.5 g under the pressure of ~0.1 GPa.

The EMF measurements of both types of cells were carried out using a Keithley Model 193 digital voltmeter with an input resistance of 10^{14} Ω and an accuracy of ~0.1 mV. The measurements were carried out during the heating and cooling of the circuits with a step of no more than 10 K. The temperature in the electrochemical cell was measured with chromel-alumel thermocouples and a mercury thermometer with an accuracy of 0.5 K. The chromel-alumel thermocouple was calibrated in advance in the 300–510 K temperature range.

The first equilibrium EMF values were obtained after holding the electrochemical cell at ~350 K for ~40-60 h, and the subsequent ones every 3–4 h after reaching the desired temperature. The system was considered to be in equilibrium if measured EMF values were constant or their variations were not significant (<0.2 mV) regardless of the direction of the temperature change at repeated measurements at a given temperature. To control the reproducibility of the cell, the EMF of each alloy was measured 2-4 times during the experiment at two constant temperatures. The reversibility of the assembled electrochemical cells and the reproducibility of the results were controlled by checking the masses and X-ray diffraction analysis of the electrodes before and after EMF measurements. The composition and mass of the electrodes during the experiment remained constant.

The analysis of the obtained temperature dependences of the EMF showed their linearity for various alloys of the Er-Te system (Fig. 15). This indicated the constancy of the phase compositions of electrode alloys in the temperature range of EMF measurements and made it possible to carry out thermodynamic calculations using the least-squares method. Calculations were performed using the computer program "Microsoft Office Excel 2010". The obtained linear equations are presented in Table 3 in the form

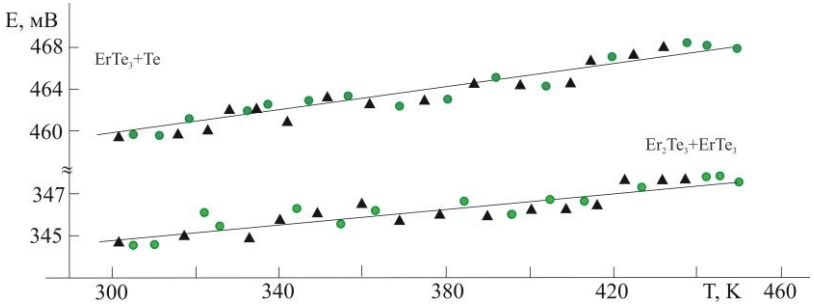

Figure 15. Temperature dependences of EMF of cells of type (2) for alloys of the Er-Te system. Green circles and black triangles are alloys of various compositions from the studied areas.

$$E = a + bT \pm t\left[\frac{S_E^2}{n} + S_b^2 (T - \overline{T})^2\right]^{1/2} \quad (3)$$

In equation (3), *a* and *b* are coefficients, *n* is the number of pairs of values E and T; $\overline{T}$ - the average temperature in K, t is Student's test, δ_E^2 and δ_b^2 are the variances of individual EMF values and the constant *b*. With the number of experimental points $n \geq 20$, and the confidence level equal to 95%, the Student's test is $t \leq 2$.

Tables 3-5 show the results for other Ln-Te systems as well.

The partial molar functions of LnTe in the alloys at 298 K (Table 4) were calculated from the temperature dependences of the EMF using the thermodynamic relations

$$\Delta\overline{G}_i = -zFE \quad (4)$$

$$\Delta\overline{H}_i = -z\left[E - T\left(\frac{\partial E}{\partial T}\right)_P\right] = -zFa \quad (5)$$

$$\Delta\overline{S}_i = zF\left(\frac{\partial E}{\partial T}\right)_P = zFb \quad (6)$$

In the equations (4)–(6), z is the charge of the potential-forming cation, F is the Faraday constant.

These values show the difference between the corresponding

Table 3

Temperature dependencies of the EMFof (1) and (2) types cells of the Ln-Te systems in the 300–450 K temperature interval

Phase area	$E, mV = a + bT \pm 2[\delta_E^2 / n + \delta_b^2 (T - \overline{T})]^{1/2}$
*GdTe-Gd_2Te_3	$991{,}5 - 0{,}089T \pm 2\left[\frac{0{,}80}{24} + 2{,}6 \cdot 10^{-5}(T - 362{,}5)^2\right]^{1/2}$
$GdTe_3$+Te	$340.582 + 0{,}0264T \pm 2\left[\frac{0.79}{30} + 1.28 \cdot 10^{-5}(T - 374.8)^2\right]^{1/2}$
$TbTe_3$+Te	$348.29 + 0.01664T \pm 2\left[\frac{0.67}{30} + 1.13 \cdot 10^{-5}(T - 375.62)\right]^{1/2}$
$TbTe_2$+$TbTe_3$	$386.99 + 0.03379T \pm 2\left[\frac{0.62}{30} + 1.05 \cdot 10^{-5}(T - 375.62)\right]^{1/2}$
Tb_2Te_3+$TbTe_2$	$425.19 + 0.05492T \pm 2\left[\frac{0.53}{30} + 8.9 \cdot 10^{-6}(T - 375.62)\right]^{1/2}$
*TbTe+Tb_2Te_3	$910.32 - 0.07214T \pm 2\left[\frac{0.69}{30} + 1.18 \cdot 10^{-5}(T - 374.89)\right]^{1/2}$
$ErTe_3$+Te	$441.4 + 0.0597T \pm 2\left[\frac{0.60}{30} + 1.02 \cdot 10^{-6}(T - 370.62)^2\right]^{1/2}$
Er_2Te_3+$ErTe_3$	$338.9 + 0.0193T \pm 2\left[\frac{0.44}{30} + 6.86 \cdot 10^{-6}(T - 377.14)^2\right]^{1/2}$
ErTe+Er_2Te_3	$979.73 - 0{,}0838T \pm 2\left[\frac{0{,}26}{24} + 8.2 \cdot 10^{-6}(T - 362{,}84)^2\right]^{1/2}$
$TmTe_3$+Te	$428.02 + 0.0446T \pm 2\left[\frac{0.65}{30} + 1.02 \cdot 10^{-5}(T - 376.7)^2\right]^{1/2}$
Tm_2Te_3+$TmTe_3$	$336.78 + 0.0032T \pm 2\left[\frac{0.74}{30} + 1.20 \cdot 10^{-5}(T - 376.7)^2\right]^{1/2}$
*TmTe+Tm_2Te_3	$924.56 - 0.0731T \pm 2\left[\frac{1.11}{30} + 1.74 \cdot 10^{-5}(T - 377.4)^2\right]^{1/2}$
Yb-Te	$102.8 - 0.1043T \pm 2\left[\frac{1.6}{20} + 1.1 \cdot 10^{-4}(T - 360.7)^2\right]^{1/2}$

* in this area, the EMF of the cell of type (1) was measured

Table 4

The partial molar functions of LnTe in the alloys at 298 K

Phase area	$-\Delta\overline{G}_{LnTe}$	$-\Delta\overline{H}_{LnTe}$	$\Delta\overline{S}_{LnTe}$
	кJ·mol^{-1}		J·mol^{-1}·K^{-1}
$GdTe_3$+Te	100.86±0.18	98.58±0.78	7.64±2.07
$TbTe_3$+Te	127.82±0.15	123.08±0.65	15.90±1.72
$TbTe_2$+$TbTe_3$	114.94±0.17	112.02±0.71	9.78±1.87
Tb_2Te_3+$TbTe_3$	102.26±0.17	100.82±0.74	4.82±1.95
$ErTe_3$+Te	132.94±0.16	127.79±0.69	17.29±1.85
Er_2Te_3+$ErTe_3$	99.78±0.14	98.11±0.58	5.6±1.52
$TmTe_3$+Te	127.75±0.17	123.90±0.70	12.91±1.85
Tm_2Te_3+$TmTe_3$	97.76± 0.18	97.49±0.75	0.93±1.98

partial molar functions of erbium for the right and left electrodes of the cell of type (2). For example,

$$\Delta\overline{Z}_{ErTe} = \Delta\overline{Z}_{Er}\ (\text{Er in alloy rich Te}) - \Delta\overline{Z}_{Er}(ErTe)$$

Z ≡ G (H). Therefore, the partial thermodynamic functions of erbium in alloys can be calculated based on the relationship

$$\Delta\overline{Z}(\text{Er in alloy}) = \Delta\overline{Z}_{Er}\ (ErTe) + \Delta\overline{Z}_{ErTe}$$

When calculating the partial thermodynamic functions of erbium in $ErTe_3$+Te and Er_2Te_3+ $ErTe_3$ alloys, we summarized the data given in Table 3 with the corresponding partial molar functions of Er in ErTe (Table 5). The results are shown in Table 5.

According to the phase diagram of the Er-Te system, these quantities are thermodynamic characteristics of the following virtual sell reactions (the substances is in crystalline state):

$$Er+3Te=ErTe_3 \quad (7)$$

$$Er+3ErTe_3=2Er_2Te_3 \quad (8)$$

$$Er+Er_2Te_3=3ErTe \quad (9)$$

According to equations (7)-(9), the standard thermodynamic functions of the formation of erbium tellurides can be calculated from the relations

$$\Delta Z^0(ErTe_3) = \Delta\overline{Z}_{Er} \quad (10)$$

$$2\Delta Z^0(Er_2Te_3) = \Delta\overline{Z}_{Er} + \Delta Z^0(ErTe_3) \quad (11)$$

$$3\Delta Z^0(ErTe) = \Delta\overline{Z}_{Er} + \Delta Z^0(Er_2Te_3) \quad (12)$$

here $\Delta Z^0 = \Delta G^0$, ΔH^0, $\Delta\overline{Z}_{Er} = \Delta\overline{G}_{Er}$, $\Delta\overline{H}_{Er}$, while standard entropy – by using the relations

$$S^0(ErTe_3) = [\Delta\overline{S}_{Er} + S^0(Er)] + 3S^0(Te) \quad (13)$$

$$2S^0(Er_2Te_3) = [\Delta\overline{S}_{Er} + S^0(Er)] + 3S^0(Te) \quad (14)$$

$$3S^0(ErTe) = [\Delta\overline{S}_{Er} + S^0(Er)] + S^0(Te) \quad (15)$$

Table 5

The partial molar functions of lanthanide in the alloys at 298 K

Phase area	$-\Delta\overline{G}_{Ln}$	$-\Delta\overline{H}_{Ln}$	$\Delta\overline{S}_{Ln}$
	кJ·mol^{-1}		J·mol^{-1}·K^{-1}
GdTe+Gd_2Te_3	279.00±0.30	287.30±1.6	-26.7±4.30
$GdTe_3$+Te	380.16±0.48	385.88±2.38	-19.18±6.37
$TbTe_3$+Te	385.10±0.33	386.58±1.40	-4.96±3.71
$TbTe_2$+$TbTe_3$	372.22±0.35	375.52±1.46	-11.07±3.86
Tb_2Te_3+$TbTe_3$	359.54±0.35	364.32±1.49	-16.03±3.94
TbTe+Tb_2Te_3	257.28±0.18	263.50±0.75	-20.88±1.99
$ErTe_3$+Te	409.30±0.28	411.38±1.29	-6.97±2.51
Er_2Te_3+$ErTe_3$	376.14±0.26	381.70±1.18	-18.65±2.18
$ErTe_3$+ErTe	276.36±0.12	283.59±0.60	-24.25±0.66
$TmTe_3$+Te	389.06±0.39	391.52±1.62	-8.25±4.27
Tm_2Te_3+$TmTe_3$	359.07±0.40	365.11±1.67	-20.23±4.40
TmTe+Tm_2Te_3	261.31±0.22	267.62±0.92	-21.16±2.42
Yb-Te	288.77±0.41	297.81±2.2	-30.20±6.10

When calculating the standard entropies of compounds, in addition to our experimental results (Table 4), we used data on the standard entropies of elemental erbium (73.14±0.63 J·mol^{-1}·K^{-1}) and tellurium (49.5±0.2 J·mol^{-1}·K^{-1}). The experimental results obtained in the dissertation were compared with the available fragmentary literature data. It is shown that our data are in better agreement with the results

obtained by the EMF method.

The obtained thermodynamic data for binary compounds (Table 6) were used to calculate the thermodynamic functions of ternary compounds of the Tl-Ln-Te systems (paragraph 5.8).

Table 6

Standard integral thermodynamic functions of binary REE tellurides

Compound	$-\Delta_f G^0(298K)$	$-\Delta_f H^0(298K)$	S^0_{298}
	кJ·mol^{-1}		J·mol^{-1}·K^{-1}
$GdTe_3$	380.2±0.5	385.9±2.4	197.3±7.8
Gd_2Te_3	756.5±2.5	768.5±10.0	249.0±8.4
GdTe	355.9±1.0	363.6±3.9	113.8±5.0
$TbTe_3$	385.1±0.3	386.6±1.4	194.9±4.8
$TbTe_2$	380.8±0.4	382.9±1.5	165.6±4.6
Tb_2Te_3	750.9±0.7	756.5±3.0	277.0±9.3
TbTe	336.1±0.3	340.0±1.3	109.9±3.9
$ErTe_3$	409.3±0.3	411.4±1.3	214.7±3.7
Er_2Te_3	784.4±0.5	793.1±2.5	269.2±6.5
ErTe	353.6±0.3	358.9±0.6	106.0±2.6
$TmTe_3$	389.1±0.4	391.5±1.6	214.3±5.1
Tm_2Te_3	748.1±0.8	756.6±3.3	268.1±9.7
TmTe	336.5±0.4	341.4±1.5	107.0±1.4
YbTe	289.0±1.0	298.0±3.0	79.0±7.0

On the example of the Tl-Tb-Te ternary system, we will briefly describe the study of ternary systems by the EMF method. Tables 7-11 also show data for other studied Tl-Ln-Te (Ln-Gd, Er, Tm) systems.

From the obtained linear equations of the temperature dependences of the EMF of the cell of type (2), and using relations (4) - (6), the partial molar Gibbs free energy, enthalpy, and entropy of TbTe in the alloys of the system were calculated (Table 7).

By combining the data obtained with the partial molar functions of Tb in TbTe, the partial molar functions of Tb in the alloys were calculated (Table 8).

Table 7
The partial molar functions of LnTe in the alloys of the Tl-Ln-Te systems at 298 K

Phase area	$-\overline{\Delta G}_{LnTe}$	$-\overline{\Delta H}_{LnTe}$	$\overline{\Delta S}_{LnTe}$
	кJ·mol^{-1}		J·mol^{1}·K^{-1}
$\delta(Tl_{9.8}Gd_{0.2}Te_6)$	236.04±0.22	217.75±0.91	61.34±2.40
$\delta(Tl_{9.6}Gd_{0.4}Te_6)$	219.89±0.21	205.81±0.88	47.22±2.31
$\delta(Tl_{9.4}Gd_{0.6}Te_6)$	208.53±0.24	198.21±1.00	34.61±2.64
$\delta(Tl_{9.2}Gd_{0.8}Te_6)$	200.78±0.21	192.33±0.89	28.34±2.35
$\delta(Tl_9GdTe_6)$	193.95±0.20	186.14±0.86	26.19±2.26
Tl_2Te_3+TlTe+$TlGdTe_2$	199.13±0.16	193.81±0.68	17.84±1.80
TlTe+Tl_9GdTe_6+$TlGdTe_2$	189.41±0.20	181.89±0.85	25.22±2.26
Tl_2Te_3 + TlTe + $TlTbTe_2$	196.17±0.24	193.01±0.97	10.61±2.54
TlTe+Tl_9TbTe_6+$TlTbTe_2$	186.40±0.24	182.30±0.98	13.77±2.58
Tl_2Te_3 + TlTe + $TlErTe_2$	197.53±0.19	190.91±0.81	22.21±2.13
TlTe+Tl_9ErTe_6 + $TlErTe_2$	188.28±0.20	183.63±0.85	16.88±2.25
Tl_2Te_3 + TlTe + $TlTmTe_2$	206.02±0.31	198.88±1.30	23.97±3.40
TlTe+Tl_9TmTe_6+$TlTmTe_2$	196.42±0.30	187.92±1.23	28.48±3.24

The standard integral thermodynamic functions of compounds of the $TlLnTe_2$ and Tl_9LnTe_6 types were calculated by the method of virtual-cell reactions. According to the solid-phase equilibria diagram (Fig. 16), the values of the partial molar functions of terbium in the TlTe-Tl_2Te_3-$TlTbTe_2$ and TlTe-Tl_9TbTe_6-$TlTbTe_2$ three-phase regions are thermodynamic functions of the following virtual-cell reactions (the substances is in the crystalline state):

$$Tb + Tl_2Te_3 = TlTe + TlTbTe_2 \qquad (16)$$

$$Tb + 3TlTe = 0.25Tl_9TbTe_6 + 0.75TlTbTe_2 \qquad (17)$$

According to the equations of these reactions, the standard thermodynamic functions for the formation of the $TlTbTe_2$ and Tl_9TbTe_6 ternary compounds can be calculated from the relations

$$\Delta_f Z^0(TlTbTe_2) = \overline{\Delta Z}_{Tb} + \Delta_f Z^0(Tl_2Te_3) - \Delta_f Z^0(TlTe), \qquad (18)$$

Table 8
The partial molar functions of Ln in the alloys of the Tl-Ln-Te systems at 298 K

Phase area	$-\overline{\Delta G}_{Ln}$	$-\overline{\Delta H}_{Ln}$	$\overline{\Delta S}_{Ln}$
	кJ·mol^{-1}		J·mol^{-1}·K^{-1}
$\delta(Tl_{9.8}Gd_{0.2}Te_6)$	515.34±0.52	504.75±2.11	35.52±5.40
$\delta(Tl_{9.6}Gd_{0.4}Te_6)$	499.19±0.51	492.81±1.98	21.40±5.31
$\delta(Tl_{9.4}Gd_{0.6}Te_6)$	487.83±0.54	485.21±2.10	8.79±5.64
$\delta(Tl_{9.2}Gd_{0.8}Te_6)$	480.08±0.51	479.33±2.00	2.52±5.35
$\delta(Tl_9GdTe_6)$	473.25±0.50	473.14±1.92	0.37±5.26
Tl_2Te_3+TlTe+$TlGdTe_2$	478.43±0.46	480.81±1.78	-7.98±4.80
TlTe+Tl_9GdTe_6 +$TlGdTe_2$	468.71±0.50	468.89±1.95	-0.60±5.26
Tl_2Te_3+TlTe+$TlTbTe_2$	453.45±0.42	456.60±1.72	-10.57±4.53
TlTe+Tl_9ErTe_6+$TlTbTe_2$	443.68±0.42	445.80±1.73	-7.11±4.57
Tl_2Te_3+TlTe+$TlErTe_2$	473.91±0.40	474.50±1.50	-2.01±2.81
TlTe+Tl_9ErTe_6+$TlErTe_2$	464.60±0.40	467.30±1.50	8.71±3.01
Tl_2Te_3+TlTe+$TlTmTe_2$	467.33±0.53	466.50±2.22	2.78±5.82
TlTe+Tl_9TmTe_6+$TlTmTe_2$	457.73±0.52	455.54±2.15	7.35±5.66

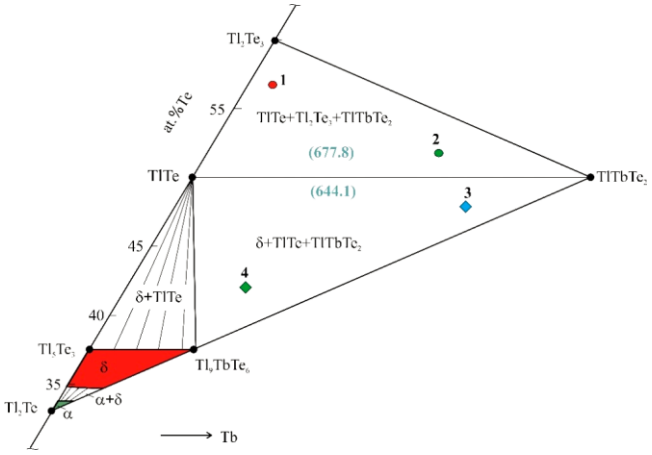

Figure 16. Solid-phase equilibria diagram of the Tl_2Te-Tl_2Te_3-$TlTbTe_2$ sub-system. The numbers indicate the values of EMF (mV) of cells of type (2) in three-phase regions.

$$\Delta_f Z^0(Tl_9TbTe_6) = 4\overline{\Delta Z}_{Tb} + 12\Delta_f Z^0(TlTe) - 3\Delta_f Z^0(TlTbTe_2) \quad (19)$$

(Z≡G, H), and standard entropy – by using the relations

$$S^0(TlTbTe_2) = \overline{\Delta S}_{Tb} + S^0(Tb) + S^0(Tl_2Te_3) - S^0(TlTe) \quad (20)$$

$$S^0(Tl_9TbTe_6) = 4\overline{\Delta S}_{Tb} + 4S^0(Tb) + 12S^0(TlTe) - 3S^0(TlTbTe_2). \quad (21)$$

In calculations using relation (18)–(21), along with the obtained experimental results (Table 8), we used the value of the standard entropy of terbium (73.51±0.42 $J \cdot mol^{-1} \cdot K^{-1}$) and thermodynamic data for the TlTe and Tl_2Te_3 compounds. The results obtained are presented in Table.9.

When performing calculations using relations (19) and (21), in addition to the partial molar functions of terbium in the three-phase region $TlTe+Tl_9TbTe_6+TlTbTe_2$ (Table 9), we used the standard integral thermodynamic functions of the $TlTbTe_2$ compound obtained by us from equations (18) and (20) (Table 9).

Table 9

Standard integral thermodynamic functions of $TlLnTe_2$ and Tl_9LnTe_6 ternary compounds

Compound	$-\Delta_f G^0(298K)$	$-\Delta_f H^0(298K)$	$S^0(298K)$,
	$kJ \cdot mol^{-1}$		$J \cdot mol^{-1} \cdot K^{-1}$
$TlGdTe_2$	524.7±1.7	526.9±3.2	227±10
$TlTbTe_2$	499.8±1.6	502.7±3.0	226.8±9.8
$TlErTe_2$	521.2±1.6	520.9±3.0	235±6.0
$TlTmTe_2$	513.6±1.7	511.6±3.7	240.6±10.8
Tl_9GdTe_6	862.8±3.7	866.3±6.3	933±20
Tl_9TbTe_6	809.1±11.0	801.3±21.5	974.8±9.8
Tl_9ErTe_6	828.8±11.2	833.8±27.0	1013±5
Tl_9TmTe_6	824.1±12.0	826.2±25.7	965.0±74.0

During the calculations of the partial and integral thermodynamic functions of binary and ternary compounds, errors were found by the method of uncertainty propagation.

The values of the standard integral thermodynamic functions of REE tellurides and ternary thallium-REE tellurides obtained by us

made it possible to calculate the standard thermodynamic functions of atomization and the relative thermodynamic stability of these compounds (paragraph 5.9). Calculations were carried out according to the relations

$$\Delta_{at}H^0(\text{comp.}) = \sum \Delta_{arr}H^0(\text{elem.}) - \Delta_f H^0(\text{comp.}) \quad (22)$$

$$\Delta_{at}S^0(\text{comp.}) = \sum S^0(\text{atomic qas}) - S^0(\text{comp.}) \quad (23)$$

$$\Delta_{at}G^0(\text{comp.}) = \Delta_{at}H^0(\text{comp.}) - T \cdot \Delta_{at}S^0(\text{comp.}) \quad (24)$$

The results obtained for ternary compounds are shown in Table 10. As can be seen, all ternary compounds are characterized by high positive values of the Gibbs free energy of atomization ΔG^0_{at} and the enthalpy of atomization ΔH^0_{at}, which are several times higher than their corresponding thermodynamic functions of formation. This is due to the fact that ΔH^0_{at} is the energy required to break all bonds in the crystal lattice with the formation of monatomic gases. High values of the atomization entropy ΔS^0_{at} are a consequence of the strong disordering of the system during the transition from the crystalline state to a mixture of monatomic gases. Almost constant values ofΔS^0_{at} within each type of compounds can be explained by the same initial and final states for each type of compounds (Table 10).

Table 10
Standard thermodynamic atomization functions for the ternary compounds of Tl-Ln-Te systems

Compound	$\Delta_{at}G^0$	$\Delta_{at}H^0$	$\Delta_{ar}S^0$, $J \cdot mol^{-1} \cdot K^{-1}$
	$kJ \cdot mol^{-1}$		
$TlGdTe_2$	283.3	436.2	513.1
$TlTbTe_2$	295.0	450.4	521.0
$TlErTe_2$	209.5	360.0	504.8
$TlTmTe_2$	138.3	286.0	495.3
Tl_9GdTe_6	3603.5	2311.3	1983.9
Tl_9TbTe_6	2083.4	2664.8	1949.8
Tl_9ErTe_6	1694.0	2261.6	1903.6
Tl_9TmTe_6	1525.5	2106.2	1947.7

We also calculated the standard thermodynamic functions of the formation for the $TlLnTe_2$ and Tl_9LnTe_6 ternary compounds from binary Tl_2Te and Ln_2Te_3 compounds.

Table 11 presents the standard thermodynamic functions of atomization, formation from elementary components and from the indicated binary compounds, for per 1 g-atom of the studied ternary compounds. As can be seen, the heat and free energy of the formation of ternary compounds from simple substances are several times lower than the values of the corresponding functions of their formation from individual atoms, and their thermodynamic functions of formation from binary compounds, in turn, are much less than the standard thermodynamic functions of formation from simple substances. This is due to the fact that the interaction of binary compounds during the formation of ternary ones is not accompanied by a significant change in the number and nature of chemical bonds. At the same time, when ternary compounds are formed from simple substances, a profound change in the nature of the chemical bond occurs - relatively weak bonds are destroyed, and much stronger "metal-non-metal" bonds are formed, which leads to a significant decrease in the energy of the system.

Table 11

Thermodynamic functions of atomization, formation from simple substances and formation from binary compounds for ternary compounds of Tl-Ln-Te systems

Compound	$\Delta_{at}G^0$	$-\Delta_fG^0$	$-\Delta G'$	$\Delta_{at}H^0$	$-\Delta_fH^0$	$-\Delta H'$
	κJ/ q-atom					
$TlGdTe_2$	334	131	27	373	132	26
$TlTbTe_2$	325	125	21	364	126	21
$TlErTe_2$	315	130	22	353	130	21
$TlTmTe_2$	290	128	25	327	128	23
Tl_9GdTe_6	202	54	8	250	54	8
Tl_9TbTe_6	198	51	5	245	50	4
Tl_9ErTe_6	197	52	5	242	52	5
Tl_9TmTe_6	190	52	6	236	52	5

At the end of the chapter (paragraph 5.10), the results of studying the magnetic properties of the Tl_9GdTe_6, Tl_9TmTe_6 compounds and the $Tl_9Bi_{0.8}Tm_{0.2}Te_6$ solid solution are presented. Graphs of the dependences of the magnetic susceptibility and the inverse value of the magnetic susceptibility on temperature are plotted. It has been established that the studied compounds are paramagnetic and obey the Curie-Weiss law (Table 12).

Table 12

Some magnetic properties for Tl_9TmTe_6, Tl_9GdTe_6 and $Tl_9Bi_{0.8}Tm_{0.2}Te_6$

Phase	χ	N, m^{-3}	μ, $A \cdot m^2$	μ/μ_B
Tl_9TmTe_6	0.00121	$1.976 \cdot 10^{27}$	$4.881 \cdot 10^{-23}$	6.95
Tl_9GdTe_6	0.00625	$1.950 \cdot 10^{27}$	$1.028 \cdot 10^{-23}$	1.11
80 мол% Tl_9BiTe_6 + 20 мол%Tl_9TmTe_6	0.00392	$1.987 \cdot 10^{27}$	$5.134 \cdot 10^{-23}$	5.53

RESULTS AND CONCLUSIONS

1. Based on the analysis of the features of the crystal structure of the Tl_5Te_3 compound and its known ternary structural analogs, the existence of new ternary compounds of the Tl_9LnTe_6 and Tl_4LnTe_3 types with the indicated structure was predicted and experimentally confirmed. A special procedure for the synthesis of these compounds was developed, with the help of which they were were synthesized in a homogeneous form and characterized. It is shown that all compounds of both types crystallize in a tetragonal structure of the Tl_5Te_3 type and melt with decomposition by peritectic reactions.
2. Using the traditional complex of experimental methods of physicochemical analysis (DTA, XRD, MSA, microhardness measurements) and EMF measurements of the concentration cells of two types, a set of new mutually consistent data on phase equilibria, crystallographic and thermodynamic properties for a number of the Tl -Ln-Te ternary systems in the range of compositions rich in thallium tellurides are obtained.
3. The nature of the physicochemical interaction in three Tl-Ln-Te ternary systems in the Tl_2Te-Tl_5Te_3-Tl_4LnTe_3 (Ln-Sm, Dy, Tm)

compositions range and three in the Tl_2Te-Tl_5Te_3-Tl_9LnTe_6 (Ln-Gd, Tb, Er) compositions range is determined. Projections of liquidus and solidus surfaces, various polythermal and isothermal cross-sections of T-x-y diagrams in the above composition regions are constructed, fields of primary phase crystallization are determined, as well as types and coordinates of non- and monovariant equilibria. It was established that all these systems, on the whole, are not independent subsystems due to the incongruent melting of the Tl_4LnTe_3 and Tl_9LnTe_6 compounds, but are stable in the subsolidus and are characterized by the formation of wide regions of solid solutions with Tl_5Te_3 structure, covering a significant part of the areas of the corresponding concentration triangles.

4. The nature of phase equilibria in the Tl-Yb-Te system in the Tl_2Te-YbTe-Te compositions range was established. Various polythermal sections and the projection of the liquidus surface were constructed. It was shown that, unlike other rare earth elements, ytterbium does not form ternary compounds with thallium.
5. To obtain multicomponent solid solutions with the Tl_5Te_3 structure, the nature of the physicochemical interaction in the Tl_5Te_3-Tl_9LnTe_6-Tl_9BiTe_6 (Ln-Sm, Gd, Tb, Er, Tm) (I), Tl_5Te_3-Tl_9LnTe_6-Tl_9SbTe_6 (Ln-Sm, Gd, Tb) (II), Tl_2Te-Tl_9LnTe_6-Tl_9BiTe_6 (Ln-Sm, Gd, Er) (III), Tl_2Te-Tl_9LnTe_6-Tl_9SbTe_6 (Ln-Sm, Gd) (IV), and Tl_4PbTe_3-Tl_9BiTe_6-Tl_9GdTe_6 (V) systems were investigated, their T-x-y phase diagrams, various horizontal and vertical sections of these diagrams are constructed. It has been established that systems (I), (II), and (V) are characterized by the formation of unlimited, and systems (III) and (IV) are characterized by the formation of wide regions of substitution solid solutions with the Tl_5Te_3 structure. On the isothermal sections of the phase diagrams, the positions of the connodes are experimentally determined, which makes it possible to obtain solid solutions with a given composition by directional crystallization from melts.
6. Thermodynamic analysis and analytical 3D modeling of the liquidus surface of the Tl_9GdTe_6-Tl_4PbTe_3-Tl_9BiTe_6 system were carried out. In particular, analytical models of T-x phase diagrams of

the Tl_9GdTe_6-Tl_4PbTe_3 and Tl_9GdTe_6-Tl_9BiTe_6 boundary systems in the "temperature-composition" coordinates were obtained. The thermodynamic mixing functions of solid solutions are determined based on the model of regular solutions of nonmolecular compounds. The data obtained confirm the thermodynamic stability of solid solutions based on the Tl_9GdTe_6, Tl_4PbTe_3, and Tl_9BiTe_6 ternary compounds over the entire concentration range and in the 300–780 K temperature range.

7. A number of "composition-property" diagrams (dependences of the crystal lattice parameters, microhardness, EMF of concentration cells, partial molar functions on composition) was constructed, the analysis of which has made it possible to establish the boundaries of the phase regions in the diagrams of solid-phase equilibria and, in particular, the homogeneity regions of the identified new phases.
8. Based on the complexes of experimental data obtained, solid solutions with a given composition were obtained in pure form, and the types and parameters of their crystal lattices were determined.
9. By EMF measurements of the concentration cells of types

   (–)Ln (s.) |glycerol+KCl+$LnCl_3$ | (Ln in alloy) (s.) (+)

   (–) LnTe (s. | glycerol + KCl + $LnCl_3$ | (Ln in alloy) (s.) (+)

   the solid-phase equilibria in Ln-Te binary and Tl-Ln-Te (Ln-Gd, Tb, Er, Tm) ternary systems and the thermodynamic properties of the telluride phases formed in them were studied. The partial thermodynamic functions ($\Delta\overline{G}$, $\Delta\overline{H}$, $\Delta\overline{S}$) of REE and their monotellurides in alloys are calculated by combining EMF measurements for cells of both types. Based on solid-state equilibria diagrams, the virtual-cell reactions were determined, with the help of which the standard thermodynamic functions of formation and the standard entropies of 13 binary and 8 ternary compounds of the studied systems were calculated. Integral thermodynamic functions of solid solutions are calculated by integrating the Gibbs-Duhem equation. Using the obtained complexes of standard integral thermodynamic functions of the formations and standard entropies of the studied compounds, their standard atomization energies and relative stability were calculated.

10. The nature of the magnetic properties of the Tl_9LnTe_6 compounds was determined. It is shown that the investigated compounds are paramagnetic and obey the Curie-Weiss law.

The main results of the dissertation work were published in the following works:

1. Бабанлы М.Б., Имамалиева С.З., Ибадова Г.И. Термодинамическое исследование системы Nd-Te методом электродвижущих сил. // Вестник БГУ, серия физико-математических наук, 2009, №4, с.5-9.
2. Babanly M.B., Tedenac J.-C., Imamaliyeva S.Z., Guseynov F.N., Dasdiyeva G.B. Phase equilibria study in systems Tl-Pb(Nd)-Bi-Te. New phases of variable composition on the base of Tl_9BiTe_6. // Journal of Alloys and Compounds, 2010, v. 491, Issue 1-2, p.230-236.
3. Имамалиева С.З., Алиев З.С., Махмудова М.А, Бабанлы М.Б., Аббасов А.С. Термодинамические свойства теллурида иттербия // Химические Проблемы, 2010, №3, с.453-456 .
4. Imamaliyeva S.Z., Babanly D.M., Babanly M.B.,Yusibov Yu.A, Sadiqov F.M. New ternary compounds Tl_9LnTe_6 type and variable composition phases on their base. / 8th International conference “Electronic processes in organic and inorganic materials”, Ivano-Frankovsk, 17-22 мая, 2010, p.83-85.
5. Бабанлы М.Б., Имамалиева С.З. Гусейнов Ф.Н, Ибрагимова Г.И. Новые фазы переменного состава в системах Tl_5Te_3-Tl_9LnTe_6-Tl_9BiTe_6 (Ln-Ce, Sm, Gd). / VI Международная научная конференция "Кинетика и механизм кристаллизации. Самоорганизация при фазообразовании", Иваново, 21-24 сентября, 2010, с.161.
6. Imamaliyeva S.Z., Guseynov F.N., Tedenac J.-C., Babanly M.B. New intermetallic phases with tl_5te_3 structure in systems Tl-Ln-Bi-Te (Ln-Ce, Sm, Gd) / XI international conference on crystal chemistry of intermetallic compounds, Lviv, 30 May- 2 June, 2010, p.19.
7. Babanly M.B., Imamaliyeva S.Z., Yusibov Yu.A., Sadiqov F.M. New ternary compounds Tl_9LnTe_6 type and variable composition

phases on their base / XIII International conference on Physics and Technology of thin films and Nanosystems, Ivano-Frankovsk, 16-21 May, 2011, p.61.
8. Бабанлы М.Б., Имамалиева С.З., Гусейнов Ф.Н., Садыгов Ф.М. Новые теллуриды таллия-РЗЭ и фазы переменного состава на их основе. / XIX Менделеевский съезд по общей и прикладной химии, т. 3, Волгоград, 25-30 сентября, 2011, с. 21.
9. Бабанлы М.Б., Имамалиева С.З., Гасанлы Т.М. Теллуриды таллия с лантаноидами и нестехиометрические фазы на их основе / Всероссийская конференция "Современные проблемы химической науки и образования", т.1, Чебоксары, 19-20 апреля, 2012, с.21.
10. Imamaliyeva S.Z., Gasanly T.M., Babanly M.B. Phase equilibria in Tl_4CuTe_3-Tl_9BiTe_6-Tl_9LnTe_6 (Ln-Nd, Sm, Gd) systems and some properties of the solid solutions / XII International conference on crystal chemistry of intermetallic compounds, Lviv, 22-26 September, 2013, p.76.
11. Imamaliyeva S.Z., Gasanova T.M., Babanly M.B. New intermetallic phase with Tl_5Te_3 structure in system Tl-Er-Bi-Te / XIV International Conference on Physics and Technology of Thin Films and Nanosystems (ICPTTFN-XIV), Ivano-Frankovsk, 20-25 May 2013, p.557.
12. Имамалиева С.З., Гасанлы Т.М. Бабанлы Д.М. Физико-химическое исследование некоторых систем типа Tl_5Te_3-Tl_9BiTe_6-Tl_9LnTe_6. / X Международное Курнаковское Совещание по физико-химическому анализу, Самара, 1 июля-5 июля, 2013, с.341-344.
13. Имамалиева С.З., Гасанлы Т.М., Искаков Р.Г., Бабанлы М.Б. Фазы переменного состава со структурой Tl_5Te_3 в системе Tl_5Te_3-Tl_9BiTe_6-Tl_9TmTe_6 / 1st International chemistry and chemical engineering conference, Baku, 17-21 April, 2013, с.300-304.
14. Imamaliyeva S.Z., Gasanly T.M., Veysova S.M., Babanly M.B. Synthesis and physico-chemical study of solid solutions based on thermoelectric Tl_9BiTe_6 /XV International scientific conference "High-Tech in Chemical engineering-2014", Moscow, 22-26

September, 2014, p.204.
15. Гасанова Т.М., Имамалиева С.З., Зейналова Г.С., Бабанлы М.Б. Фазовые диаграммы и кристаллизация твердых растворов в системе Tl_5Te_3-Tl_9BiTe_6-Tl_9LnTe_6 (Ln-Tb, Dy) / VIII Международная научная конференция "Кинетика и механизм кристаллизации. Кристаллизация как форма самоорганизации вещества", Иваново, 24-27 июня, 2014, с.140.
16. Gasanly T.M., Imamaliyeva S.Z. Phase equilibria in Tl_5Te_3-Tl_9SbTe_6-Tl_9LnTe_6 (Ln-Sm, Gd) systems and some properties of solid solutions / 1st International scientific conference of young scientists and specialists "The role of multidisciplinary aproch in soluti of actual problems of fundamental and applied sciences (earth, technical and chemical)" Baku, 15-16 October, 2014, p. 414.
17. Imamaliyeva S.Z., Mashadiyeva L.F., Zlomanov V.P., Babanly M.B. Phase equilibria in the Tl_2Te-YbTe-Te system // Inorganic materials, 2015, v.50, №12, p.1237-1242.
18. Imamaliyeva S.Z., Gasanly T.M.,Sadygov F.M.,Babanly M.B. Phase diagram of the Tl_2Te-Tl_9TbTe_6 system // Azerbaijan Chemical Journal, 2015, №3, p.93-97.
19. Gasanly T.M., Amiraslanov I.R.,Imamalieva S.Z., Babanly M.B. New ternary compounds of Tl_9LnTe_6 type and solid solutions on their base / International Conference Applied Mineralogy and Advanced materials, AMAM- 2015, Castellaneta Marina, 7-12 June, 2015, p.129.
20. İmamaliyeva S.Z., Gasanly T.M., Sadygov F.M., Babanly M.B. Features of phaseformation in the $Tl_5Te_3(Tl_2Te)$-Tl_9LnTe_6-$Tl_9B^VTe_6$ systems/ 1st International Turkic World Conference on Chemical Sciences and Technologies, Sarajevo, 27 October-1 November, 2015, p.304.
21. Imamalieva S.Z., Gasanly T.M., Sadygov F.M., Babanly M.B. Phase equilibria in the Tl_2Te-Tl_9GdTe_6-Tl_9SbTe_6 system / 5th international conference "HighMatTech", Kiev, 5-8 October, 2015, p. 49.
22. Imamalieva S.Z., Gasanly T.M., Mehdiyeva I.F., Babanly M.B. Fabrication and some properties of solid solutions in the Tl_5Te_3-

Tl_9GdTe_6 system / XV International Conference on Physics and Technology of Thin Films and Nanosystems (ICPTTFN-XV), Ivano-Frankovsk, 11-16 May, 2015, p.358.
23. Имамалиева С.З.,Гасанлы Т.М.,Садыгов Ф.М., Бабанлы М.Б. Твердые растворы в системе Tl_5Te_3-Tl_9ErTe_6 / Всероссийская научная конференция с международным участием «II Байкальский материаловедческий форум», Улан-Уде, 29 июня-5 июля, 2015, ч.1, с.67.
24. Имамалиева С.З., Гасанлы Т.М., Садыгов Ф.М., Бабанлы М.Б. Изучение области гомогенности и термодинамических свойств методом Tl_9GdTe_6 ЭДС / VII Международная научная конференция "Современные методы в теоретической и экспериментальной электрохимии", Плес, 21-25 сентября, 2015, с.117.
25. Имамалиева С.З., Гасанлы Т.М., Мехдиева И.Ф., Садыгов Ф.М. Синтез и исследование нестехиометрических фаз в системах Tl_5Te_3-$Tl_9Sm(Tm)Te_6$ / Республиканская научная конф., посвященная 90-летнему юбилею академика Шахтахтиского Т.Н., Баку, 2015, с.123.
26. Имамалиева С.З. Т-х диаграмма системы Tl_2Te-Tl_9TmTe_6 // Международный журнал прикладных и фундаментальных исследований, 2016, №6 (часть 3), с.451-455.
27. Имамалиева С.З. Т-х диаграмма системы Tl_9TmTe_6-Tl_9BiTe_6// Международный журнал прикладных и фундаментальных исследований, 2016, №7 (часть 5), с.792-795.
28. Imamaliyeva S.Z., Gasanly T.M., Mehdiyeva I.F., Sadygov F.M., Babanly M.B. Phase relations in the Tl_5Te_3-Tl_2Te-Tl_9LnTe_6 (Ln-Gd, Tb) systems and some properties of solid solutions / 2nd International Turkic World Conference on Chemical Sciences and Technologies, Skopje, October 26-30, 2016, p.241.
29. Имамалиева С.З., Гасанлы Т.М., Садыгов Ф.М., Бабанлы М.Б. Твердофазные равновесия в системе Tl_2Te-Tl_5Te_3-Tl_9TbTe_6 и термодинамические свойства Tl_9TbTe_6 / XI международное Курнаковское совещание по физико-химическому анализу в рамках XX менделеевского съезда по общей и прикладной химии, Воронеж, 27 июня-1 июля, 2016, с.136-138.

30. Имамалиева С.З., Алекберзаде Г.И., Агаев Ф.Г., Бабанлы М.Б. Твердые растворы замещения в системе Tl_4PbTe_3-Tl_9BiTe_6-Tl_9GdTe_6 / Всероссийская конференция "Химия твердого тела и функциональные материалы – 2016", Екатеринбург, 20-23 сентября 2016, с.142-143.
31. Имамалиева С.З., Алекберзаде Г.И., Агаев Ф.Г., Бабанлы М.Б. Фазовая диаграммы системы Tl_4PbTe_3-Tl_9BiTe_6-Tl_9GdTe_6 / Республиканская научная конференция, посвященная 80-летнему юбилею Института катализа и неорганической химии, Баку, 15-16 ноября 2016, с.51-52.
32. Imamaliyeva S.Z., Mekhdiyeva I.F.,Gasymov V.A., Babanlı M.B. Phase equilibria in the Tl_5Te_3-Tl_9BiTe_6-Tl_9TmTe_6 section of the Tl-Bi-Tm-Te quaternary system // Materials Research, 2017, 20(4), p.1057-1062.
33. Imamaliyeva S.Z., Gasanly T.M., Gasymov V.A., Babanlı M.B. Phase equilibria and some properties of solid solutions in the Tl_5Te_3-Tl_9SbTe_6-Tl_9GdTe_6 system // Acta Chimica Slovenia, 2017, v.64, p.221–226.
34. Imamaliyeva S.Z., Mekhdiyeva I.F., Amiraslanov I.R., Babanlı M.B. Phase equilibria in the Tl_2Te-Tl_5Te_3-Tl_9TmTe_6 section of the Tl-Tm-Te system // Phase equilibria and diffusion, 2017, v.38, issue 5, p. 764–770.
35. Imamaliyeva S.Z., Gasanly T.M., Zlomanov V.P., Babanly M.B. Phase equilibria in the Tl_2Te-Tl_5Te_3-Tl_9TbTe_6 system // Inorganic Materials, 2017, v. 53, №. 4, p. 361–368.
36. Imamaliyeva S.Z., Gasanly T.M., Zlomanov V.P., Babanly M.B. Phase equilibria in the Tl_5Te_3-Tl_9BiTe_6-Tl_9TbTe_6 system // Inorganic Materials, 2017, v. 53, № 7, p 685-689.
37. Imamaliyeva S.Z., Gasymov V.A, Babanlı M.B. Phase equilibria in the Tl_2Te-Tl_5Te_3-Tl_9SmTe_6 system // The Chemist, 2017, v.90, №1, p.1-6.
38. Imamaliyeva S.Z., Gasanly T.M., Amiraslanov I.R. Babanlı M.B. Phase relations in the Tl_5Te_3-Tl_9SbTe_6-Tl_9TbTe_6 system // Chemistry & Chemical Technology, 2017, v.11, №4, p.415-419.
39. Imamaliyeva S.Z., Gasanly T.M., Gasymov V.A., Babanly M.B.

Phase relations in the Tl_9SbTe_6-Tl_9GdTe_6 and Tl_9SbTe_6-Tl_9TbTe_6 systems // Chemical Problems, 2017, №3, p.241-247.
40. Imamaliyeva S.Z., Gasanly T.M., Mahmudova M.A., Sadygov F.M. Thermodynamic properties of GdTe compound // Azerbaijan Journal of Physics, 2017, v.XXIII, №.4, p.19-21.
41. Мехдиева И.Ф., Имамалиева С.З., Мирзоева Р.Дж, Бабанлы М.Б. Соединения типа Tl_9LnTe_6- новый класс термоэлектрических материалов с аномально низкой теплопроводностью / IX Международная научно-техническая конференция микро- и нанотехнологии в электронике. Нальчик, 29 мая - 3 июня, 2017, с.108-112.
42. Imamaliyeva S.Z., Babanly D.M., Tagiev D.B., Babanly M.B. Physicochemical Aspects of Development of Multicomponent Chalcogenide Phases Having the Tl_5Te_3 Structure: A Review // Russian Journal of Inorganic Chemistry, 2018, v.63, №13, p.1704-1027.
43. Имамалиева С.З. Фазовые диаграммы в разработке теллуридов таллия-РЗЭ со структурой Tl_5Te_3 и многокомпонентных фаз на их основе // Конденсированные среды и межфазные границы, 2018, т. 20, № 3, с. 332–347.
44. Imamaliyeva S.Z., Gasanly T.M., Sadygov F.M., Babanly M.B. Phase diagram of the system Tl_2Te-Tl_5Te_3-Tl_9GdTe_6 // Russian Journal of Inorganic Chemistry, 2018, v.63, №2, p.262-269.
45. Imamaliyeva S.Z., Babanly D.M., Gasanly T.M., Tagiev D.B., and Babanly M. B. Thermodynamic Properties of Tl_9GdTe_6 and $TlGdTe_2$// Russian Journal of Physical Chemistry A, 2018, v. 92, №11, p. 2111–2117.
46. Imamaliyeva S.Z., Mekhdiyeva I.F., Amiraslanov I.R., Babanly M.B. Investigation of the Tl_2Te-Tl_9ErTe_6 and Tl_5Te_3-Tl_9ErTe_6 systems // Applied Solid State Chemistry, 2018, №4(5), p.76-81 .
47. Mekhdiyeva I.F., Babanly K.N., Mahmudova M.A., Imamaliyeva S.Z. The Tl_9ErTe_6-Tl_9BiTe_6 system and some properties of solid solutions // Azerbaijan Chemical Journal, 2018, №2, p.80-86.
48. Imamaliyeva S.Z., Alakbarzade G.I., Salimov Z.E., Izzatli S.B., Jafarov Ya.I., Babanly M.B. The Tl_4PbTe_3-Tl_9GdTe_6-Tl_9BiTe_6

izopleth section of the Tl-Pb-Bi-Gd-Te system // Chemical Problems, 2018, №4(16), p. 496-504.
49. Имамалиева С.З., Мирзоева Р.Дж., Султанова С.Г., Имамалиев А.Р., Бабанлы М.Б. Твердофазные равновесия в системах Tl_2Te-Tl_2Te_3-$TlLnTe_2$ и термодинамические свойства соединений $TlLnTe_2$ и Tl_9LnTe_6 (Ln-Nd, Gd) / VIII Всероссийская конференция с международным участием «Физико-химические процессы в конденсированных средах и на межфазных границах – ФАГРАН-2018», Воронеж, 8-11 октября 2018, с.425.
50. Мехдиева И.Ф., Имамалиева С.З., Шукурова Г.М., Бабанлы М.Б. Твердые растворы со структурой Tl_5Te_3 в системе Tl-Bi-Er-Te / VIII Всероссийская конференция с международным участием «Физико-химические процессы в конденсированных средах и на межфазных границах – ФАГРАН-2018», Воронеж, 8-11 октября 2018, с.438-440.
51. Imamaliyeva S.Z., Mekhdiyeva I.F., Gasymov V.A., Babanly M.B. Tl–Bi–Er–Te System in the Composition Region Tl_2Te–Tl_9BiTe_6–Tl_9ErTe_6 // Russian Journal of Inorganic Chemistry, 2019, v.64, №7, p.907-913.
52. Mekhdiyeva I.F., Babayeva P.H., Zlomanov V.P., Imamaliyeva S.Z. // Phase equilibria in the Tl_2Te-Tl_5Te_3-Tl_9ErTe_6 system // New Materials, Compounds and Applications, 2019, №4, p.142-149.
53. Mekhdiyeva I.F., Imamaliyeva S.Z., Sultanova S.Q., Babanly M.B. Thermodynamic properties of the Tl_9TmTe_6 and $TlTmTe_2$ compounds / XXII International Conference on Chemical Thermodynamics in Russia, Saint Petersburg, June 19-23, 2019, p.203.
54. Мехдиева И.Ф., Имамалиева С.З., Зломанов В.П., Бабанлы М.Б. Твердые растворы со структурой Tl_5Te_3 в системе Tl_2Te-Tl_9BiTe_6-Tl_9ErTe_6 / "Müasir təbiət və iqtisad elmlərinin aktual problemləri" Beynəlxalq elmi konrfansı, Gəncə, Azərbaycan, 02-03 may, 2019, s. 22-25.
55. Imamaliyeva S.Z., Mekhdiyeva I.F., Babanly D.M., Zlomanov V.P., Tagiyev D.B., Babanly M.B. Solid-phase equilibria in the Tl_2Te-Tl_2Te_3-$TlErTe_2$ system and thermodynamic properties of

Tl_9ErTe_6 and $TlErTe_2$ compounds // Russian Journal of Inorganic Chemistry, 2020, v.65, №11, p.1762-1769.
56. Imamaliyeva S.Z., Mehdiyeva I.F., Taghiyev D.B., Babanly M.B. Thermodynamic investigations of the erbium tellurides by EMF method // Physics and Chemistry of Solid State, 2020, v.21, №2, p. 312-318.
57. Imamaliyeva S.Z., Tl_4GdTe_3 and Tl_4DyTe_3 – Novel Structural Tl_5Te_3 Analogues // Physics and Chemistry of Solid State, 2020, v.21, №3, p. 492-495.
58. Imamaliyeva S.Z., Babanly D.M., Zlomanov V.P., Taghiyev D.B., Babanly M.B. Thermodynamic properties of terbium tellurides // Condensed Matter and Interphases, 2020, №4, p. 453-459.
59. Imamaliyeva S.Z. New thallium tellurides with rare earth elements// Condensed Matter and Interphases. 2020, №4, p.460-465
60. Imamaliyeva S.Z., Amiraslanov I.R, Shevelkov A.V., Babanly M.B. Compounds of Tl_4LnTe_3 type – new structural analogues of Tl_5Te_3 / International Conference On Actual Problems Of Chemical Engineering, dedicate to the 100^{th} anniversary of the azerbaijan state oil and industry university, Baku, 24-25 December, 2020, p.143.
61. Imamaliyeva S.Z., Babanly D.M., Qasymov V.A., Babanly M.B. Solid-phase relations in the Tl_2Te-Tl_2Te_3-$TlTbTe_2$ system and thermodynamic properties of thallium-terbium tellurides // JOM, 2021, v.73, p.1503–1510.
62. Imamaliyeva S.Z., Mehdiyeva I.F., Qasymov V.A., Babanly D.M., Taghiyev D.B., Babanly M.B. Solid-Phase Equilibria and Thermodynamic Properties of Phases in the Tm–Te System // Russian Journal of Physical Chemistry A, 2021, v.95, №5, p. 926-932.
63. Imamaliyeva S.Z., Babanly D.M., Qasymov V.A., Babanly M.B. New thallium dysprosium tellurides and phase equilibria in the Tl_2Te-Tl_5Te_3-Tl_4DyTe_3 system // Russin Journal of Inogranic chemistry, 2021, v. 66, №4, p.558-568
64. Imamaliyeva S.Z., Mekhdiyeva I.F., Jafarov Y.I., Babanly M.B. Thermodynamic study of the thallium-thulium tellurides by EMF

method // Bulletin of the Karaganda University. "Chemistry" series, 2021, v.21, №2, pp. 43-52.
65. Imamaliyeva S.Z. Thermodynamic properties of the $GdTe_3$ compound // Physics and Chemistry of Solid State, 2021, v.22, №2, pp.420-425.
66. Imamaliyeva S.Z. Phase equilibria along the TlTe-$TlTmTe_2$ AND Tl_2Te_3-$TlTmTe_2$ sections of the Tl-Tm-Te system // Azerbaijan Chemical Journal, 2021, №3, p.54-58.
67. Imamaliyeva S.Z., Mamedov A.N., Babanly M.B. Modeling the phase diagram of the Tl_9GdTe_6 -Tl_4PbTe_3 -Tl_9BiTe_6 system // New Materials, Compounds and Applications, 2021, №2, p.79-86.
68. Imamaliyeva S.Z. Thermodynamic properties of some rare earth metals tellurides. / 10eh Rostocker International Conference: "Thermophysical Properties for Technical Thermodynamics", Rostock, 9-10 September, 2021, p.115.
69. Imamaliyeva S.Z. Phaseformation and regularities of phase equilibria in the Tl-Ln-Te systems / 1st International Congress Of Natural Sciences (ICNAS-2021), Erzurum, 10-12 September 2021, p.102
70. Imamaliyeva S.Z., Sultanova S.G., Mirzoyeva A.M., Mamedov A.N. 3D modeling of the phase diagrams of the Tl_9GdTe_6 -$2Tl_4PbTe_3$ and Tl_9GdTe_6-Tl_9BiTe_6 systems / XI Международная научная конференция "Кинетика и механизм кристаллизации. Кристаллизация и материалы нового поколения", Иваново, 20-24 сентября, 2021, с.228.

The defense will be held on 02 June 2022 at 10^{00} at the meeting of the Dissertation council ED1.15 of Supreme Attestation Commission under the President of the Republic of Azerbaijan operating at acad.M.Naghiyev Institute of Catalysis and Inorganic Chemistry

Address: H.Javid, 113, AZ-1143, Baku, Azerbaijan

The dissertation is accessible at the acad.M.Naghiyev Institute of Catalysis and Inorganic Chemistry library.

Electronic versions of dissertation and its abstract are available on the official website of the at acad.M.Naghiyev Institute of Catalysis and Inorganic Chemistry www.kqkiamea.az

Abstract was sent to the required addresses on 27 April 2022

Signed for printing: 21.04.2022

Paper format: 60x84$^{1/16}$

Volume: 82 191 characters

Number of hard copies: 20